ChemMedChem

Chemistry Europe
European Chemical Societies Publishing

Accepted Article

Title: Design, synthesis, radiosynthesis and biological evaluation of Fenretinide analogues as anticancer and metabolic syndrome-preventive agents

Authors: Matteo Zanda, Ilaria Patruno, Dawn Thompson, Sergio Dall'Angelo, Albert D. Windhorst, Danielle J. Vugts, Alex J. Poot, and Nimesh Mody

To be cited as: *ChemMedChem* 10.1002/cmdc.202000143

Link to VoR: https://doi.org/10.1002/cmdc.202000143

WILEY-VCH

WILEY-VCH

FULL PAPER

Design, synthesis, radiosynthesis and biological evaluation of Fenretinide analogues as anticancer and metabolic syndrome-preventive agents

Ilaria Patruno,[a] Dawn Thompson,[a] Sergio Dall'Angelo,[a] Albert D. Windhorst,[b] Danielle J. Vugts,[b] Alex J. Poot,[b] Nimesh Mody,*[a] Matteo Zanda*[a],[c],[§]

[a] Ilaria Patruno, Dr. Dawn Thompson, Dr. Sergio Dall'Angelo, Dr. Nimesh Mody, Prof. Dr. Matteo Zanda
Institute of Medical Sciences, University of Aberdeen, Aberdeen, Scotland, AB25 2ZD, UK
E-mail: n.mody@abdn.ac.uk, m.zanda@lboro.ac.uk
[b] Prof. Dr. Albert D. Windhorst, Dr. Danielle J.Vugts, Dr Alex J. Poot
Amsterdam UMC, VU University Medical Center, Cancer Center Amsterdam, dept. Radiology and Nuclear Medicine, De Boelelaan 1117, 1081 HV Amsterdam, The Netherlands
[c] Prof. Dr. Matteo Zanda
C.N.R.-SCITEC, via Mancinelli 7, 20131 Milan (Italy)
[§] Prof. Dr. Matteo Zanda
Current address: Loughborough University, School of Science, Centre for Sensing and Imaging Science, Sir David Davies Building, Loughborough LE11 3TU, UK.

Supporting information for this article can be found under XXX.

Abstract: Fenretinide (4-HPR) is a synthetic derivative of All-*Trans*-Retinoic Acid (ATRA) characterised by improved therapeutic properties and toxicological profile relative to ATRA. 4-HPR has been mostly investigated as an anti-cancer agent, but recent studies evidenced its promising therapeutic potential for preventing metabolic syndrome. Several biological targets are involved in 4-HPR's activity, leading to the potential use of this molecule for treating different pathologies. However, although 4-HPR displays quite well-understood multi-target promiscuity with regards to pharmacology, interpreting its precise physiological role remains challenging. In addition, despite promising results *in vitro*, the clinical efficacy of 4-HPR as a chemotherapeutic agent has not been satisfactory so far. Here we describe the preparation of a library of 4-HPR analogues, followed by the biological evaluation of their anti-cancer and anti-obesity/diabetic properties. The click-type analogue **3b** showed good capacity to reduce the amount of lipid accumulation in 3T3-L1 adipocytes during differentiation. Furthermore, it showed an IC_{50} = 0.53±0.8μM in cell viability tests on breast cancer cell line MCF-7, together with a good selectivity (SI = 121) over non-cancerous HEK293 cells. Thus, **3b** was selected as a potential PET tracer to study retinoids *in vivo* and the radiosynthesis of [^{18}F]**3b** was successfully developed. Unfortunately, the stability of [^{18}F]**3b** turned out to be insufficient for pursuing imaging studies.

Introduction

Fenretinide, or *N*-(4-hydroxyphenyl)retinamide (4-HPR), is a synthetic derivative of All-*Trans*-Retinoic Acid (ATRA), which is the most active metabolite of vitamin A (Figure 1).[1]

ATRA has important physiological functions including roles in vision, regulation of cell proliferation and differentiation, growth of bone tissue, immune function and activation of tumor suppressor genes.[2] However, the chronic administration of therapeutic concentrations of ATRA leads to hepatic toxicity, limiting its use in therapy. The basic structure of ATRA and other retinoid molecules consists of an alicyclic end group, a polyene spacer chain and a polar end group.[3] Conversely, in the structure of 4-HPR the polar carboxylate end group is replaced by a 4-hydroxyphenyl carboxamide. Thanks to this chemical modification, 4-HPR preferentially accumulates in fat tissue over liver, displaying an improved toxicological profile. Therefore, 4-HPR has been investigated for decades as an anti-cancer agent, showing to be more potent than ATRA in inhibiting cancer cell proliferation.[4] Moreover, recent studies reported the potential therapeutic properties of 4-HPR for the treatment of metabolic syndrome, showing a leaner phenotype and improved glucose handling in mouse models of obesity treated with 4-HPR.[5–7]

Various mechanisms of action are involved in the beneficial effects of 4-HPR; these include for example the capacity of 4-HPR to induce apoptosis through generation of radical oxygen species (ROS) or its ability to reduce ceramides (Cer) levels via the inhibition of the *de novo* synthesis pathway.[8] In addition, 4-HPR may act via a mechanism ATRA-dependent in the inhibition of adipocyte differentiation.[9] Specifically, ATRA blocks adipogenesis when introduced at early stage of differentiation by inhibiting the transcription of CAAT/enhancer binding protein (C/EBPβ) which regulates adipogenesis and adipocyte biology.[5,10]

Earlier studies reported some 4-HPR derivatives with a reduced IC_{50} in the inhibition of cancer cell proliferation compared to 4-HPR.[11-18] However, none of the 4-HPR derivatives previously synthesized showed a marked increase in potency relative to 4-HPR, with IC_{50} values still in the micromolar range. Importantly, to the best of our knowledge, the only reported structure activity relationship (SAR) study focused on the use of 4-HPR derivatives in metabolic syndrome relies on 4-HPR derivatives designed as disrupters of the protein-protein interactions between Serum Retinol Binding Protein and Transthyretin in order to prevent insulin resistance and diabetes.[19] Lastly, a comprehensive study on 4-HPR's SAR investigating both the anti-cancer and the anti-obesity/diabetic properties has not been reported to date.

In this study we synthesized a library of 4-HPR analogues using a SAR approach to determine which chemical groups are important for the biological activity of 4-HPR, in order to shed further light on its pharmacological mechanism *in vitro*. Our final goal was to identify 4-HPR analogues with improved anti-cancer activity and/or anti-obesity and anti-diabetic properties relative to the parent molecule. Furthermore, we designed new 4-HPR-click-type analogues to be used as candidate PET imaging tracers for studying retinoids *in vivo*. This was deemed to be important, because despite the promising results obtained *in vitro* on several cancer cell lines,[20,21] the efficacy of 4-HPR was shown to be reduced *in vivo*. This is likely due to its low bioavailability, which decreases the amount of drug that effectively reaches the tumour *in vivo*.[22] The use of radiolabeled 4-HPR analogues might represent a powerful tool to further investigate the pharmacological profile of 4-HPR and analogues *in vivo*, thus facilitating the development of new retinoid drug candidates.

Herein, we report (1) the design and synthesis of a library of 4-HPR analogues (**1a-j**, **2a-d**, **3a-b**); (2) the capacity of analogues **2b** and **3b** to selectively inhibit MCF-7 cell viability with a reduced IC_{50} relative to 4-HPR and their biological characterization; (3) the capacity of analogues **2b**, **2d** and **3b** to reduce lipid accumulation during 3T3-L1 adipocytes differentiation; (4) the radiosynthesis of the candidate PET tracer [^{18}F]**3b**.

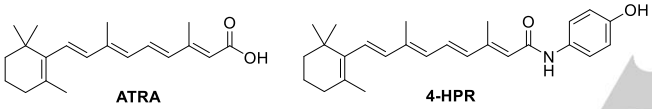

Figure 1. Chemical structure of ATRA and 4-HPR.

Results and Discussion

CHEMISTRY

4-HPR analogues 1a-j and 2a-b

To perform a SAR study on the phenol ring of 4-HPR, the ATRA scaffold was maintained intact. To this end, different functions (R^1, R^2, R^3) such as halogens, polar groups and non-polar groups were added to the aromatic ring. Furthermore, in analogues **1f**, **1h** and **2a** a -CH_2- spacer between the amide group and the aromatic ring was introduced. The synthesis of 4-HPR analogues **1a-j** and **2a-d** relied on an amide coupling between ATRA (commercially available) and benzylamine or aniline derivatives. Different coupling agents such as 2-Ethoxy-1-ethoxycarbonyl-1,2-dihydroquinoline (EEDQ), N,N'-dicyclohexylcarbodiimide (DCC) and 1-Ethyl-3-(3-dimethylaminopropyl)carbodiimide (EDC) were screened. However, we obtained the best yields – along with the most effective work-up and purification – with the widely used coupling reagent 1-[Bis(dimethylamino)methylene]-1*H*-1,2,3-triazolo[4,5-*b*]pyridinium 3-oxid hexafluorophosphate (HATU).[23] The base used was generally DIPEA, but 2,4,6-collidine was used for compounds **2a-d** in order to avoid phenolic deprotonation (Scheme 1 and Table 1).

The preparation of these new 4-HPR derivatives was straightforward, leading to compounds **1a-j** and **2a-d** in good yield, whereas the main issue was the stability of these derivatives.

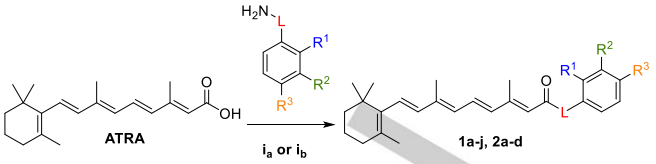

Scheme 1. Synthesis of derivatives **1a-j** and **2a-d**. Reagents and conditions: i_a) HATU, DIPEA, DCM, r.t., overnight. i_b) HATU, 2,4,6-collidine, DCM, r.t., overnight.

Table 1. Derivatives **1a-j** and **2a-d**.

Compound	L	R^1	R^2	R^3	yield
1a	none	H	H	F	60%
1b	none	H	CF_3	H	67%
1c	none	H	*t*-Bu	H	63%
1d	none	H	H	Ph	60%
1e	none	H	H	Cl	65%
1f	-CH_2-	H	H	H	89%
1g	none	H	Cl	H	70%
1h	-CH_2-	Cl	H	Cl	88%
1i	none	H	H	NO_2	50%
1j	none	OCH_3	H	H	85%
2a	-CH_2-	H	H	OH	60%
2b	none	H	F	OH	60%
2c	none	CH_3	H	OH	60%
2d	none	H	Cl	OH	62%

Literature reports have shown that retinoids – due to the presence of the all-*trans* conjugated double bonds system – are rather unstable and can be readily oxidised and/or isomerised to related compounds, especially in the presence of oxidants including air, light, and excessive heat.[24] This was confirmed for most of the newly synthesised 4-HPR derivatives. We observed that a faster degradation occurred at temperatures higher than 40 °C or when 0.1% TFA was used as an additive for preparative RP-HPLC. In this specific case the molecules were fully decomposed after solvent evaporation. In order to preserve their stability, the 4-HPR analogues were therefore handled in dim light, using labware wrapped with aluminium foil and avoiding any excess of heating or low pH conditions at each stage of synthesis and purification.

4-HPR click-type analogues 3a and 3b

New 4-HPR click-type analogues were designed as potential fluorine-18 PET tracers. In doing so, we firstly considered the stability of the ATRA scaffold which is amenable to degradation particularly when subjected to heating. Radiofluorination is usually performed at high temperature, thus the direct introduction of fluorine-18 onto 4-HPR scaffold was not deemed to be a viable strategy. Conversely, the synthetic strategy based on the Cu(I)-catalyzed Azide-Alkyne Cycloaddition (CuAAC) (Figure 2) which is widely used for the labelling of sensitive molecules with radioactive or fluorescent probes,[25] provided a more promising

alternative to deliver 4-HPR scaffolds compatible with PET imaging applications. In addition, 1,2,3-triazoles are often used in medicinal chemistry because of their advantageous physicochemical features such as polarity, rigidity, ability to act as both hydrogen bond donors and acceptors, as well as marked stability under hydrolytic, oxidative and reductive conditions.[26]

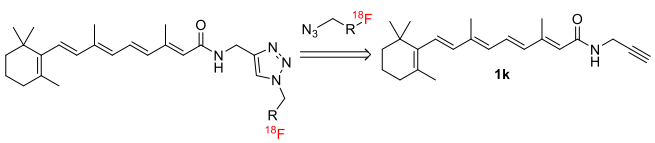

Figure 2. Retrosynthetic CuAAC strategy for generating 4-HPR analogues.

The click-type derivatives **3a** and **3b** were successfully synthesised starting from ATRA, which was coupled with propargylamine using HATU and DIPEA. The propargylamide derivative **1k** was then reacted with an azide (obtained in turn from benzyl bromide or 4-fluoro-bromobutane and sodium azide) at room temperature via the CuAAC to give the triazole derivatives **3a** and **3b** in high yield after Flash Chromatography (FC) purification (80-90%) (Scheme 2).

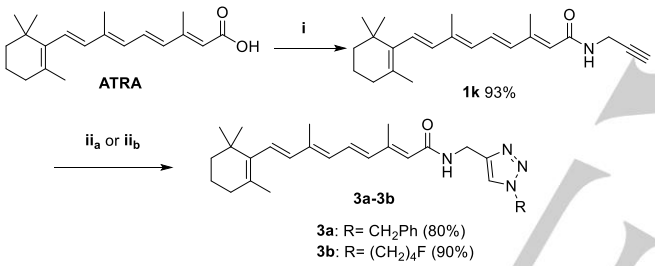

Scheme 2. Synthesis of 4-HPR analogues **3a** and **3b**. Reagents and conditions: i) propargylamine, HATU, DIPEA, DCM, r.t., overnight. ii_a) benzylazide, $CuSO_4$, Sodium Ascorbate in *t*-BuOH/H_2O, r.t., 3h. ii_b) 1-azido-4 fluorobutane, $CuSO_4$, sodium ascorbate in *t*-BuOH/H_2O, r.t., overnight.

IN VITRO STUDY AND SAR

Cell viability assays to evaluate the anti-cancer activity

The capacity of compounds **1a-j**, **2a-d** and **3a-b** to inhibit cell viability after treatment was screened on the breast cancer cell line MCF-7 using the MTT assay. It was found that several compounds inhibited cell viability of MCF-7 cells by 50% when incubated for 24 hours at micro to nanomolar concentrations (Table 2). Specifically, it was observed that the introduction of a methyl group or a chlorine atom on the 4-HPR phenol ring (**2c**, **2d**) did not influence the activity of the parent molecule (the IC_{50} values were comparable). Conversely, the meta substitution with a fluorine atom (**2b**) reduced the IC_{50} from 10.4 µM to 56 nM, strongly increasing the capacity of inhibiting MCF-7 cells viability. The absence of a group in para position (**1b**, **1c**, **1g**, **1j**) instead reduced the potency of the new compounds. Replacement of the OH with a halogen (**1a**, **1e**) did not alter the activity, while the replacement with a non-polar group – such as a phenyl ring, **1d** – reduced the IC_{50} to 96 nM. Lastly, when the OH was replaced by a nitro group (**1i**) or a spacer (-CH_2-) was introduced between the amide group and the aromatic ring (**1f**, **1h**, **2a**) the cytotoxicity was dramatically reduced (IC_{50} > 50 µM). Interestingly, we observed that replacement of the 4-HPR phenyl ring with a triazole ring preserved – or increased, as in compound **3b** – the capacity to inhibit MCF-7 cell viability. Specifically, we recorded for compounds **3a** and **3b** IC_{50} values of 22.6 µM and 0.53 µM, respectively. In addition, our data indicated that 4-HPR and some 4-HPR derivatives exhibited higher capacity to reduce cancer cell viability than ATRA itself (IC_{50} = 82.9 µM), implying an ATRA-independent mechanism as previously reported.[4] From these results it was concluded that the addition of the bulky 4-hydroxyphenyl group to the ATRA scaffold is not only responsible for the improved toxicological profile, but also for the increased anticancer activity of the molecule. Compounds **1d**, **2b**, **2c**, **2d** and **3b** were subsequently tested for their selectivity towards non-cancerous cells HEK293. The MTT assay was repeated on HEK293 cells after treatment with selected compounds. It was found that – as for 4-HPR – compounds **2b**, **2c**, **2d** and **3b** had a reduced capacity to inhibit HEK293 cell viability relative to the treatment at the same concentrations on MCF-7 cells (Figure 3). Interestingly, while **2c** and **2d** showed the same selectivity when compared to 4-HPR, **2b** and **3b** were more selective, displaying a Selectivity Index (SI) of 666 and 121 respectively (Table 2). On the contrary, compound **1d** had a non-specific cytotoxic activity.

Table 2. IC_{50} of ATRA, 4-HPR and compounds **1a-j**, **2a-d, 3a-b** concerning the inhibition of cell viability measured on MCF-7 and HEK293 cells and relative SI.

Compound	IC_{50} MCF-7[a] [µM]	IC_{50} HEK293[a] [µM]	SI[b]
ATRA	82.9±3.8	-	-
4-HPR	10.4±3.0	49.3±17	5
1a	9.3±1.7	-	-
1b	60.1±43	-	-
1c	20.8±11	-	-
1d	0.096±0.05	0.047±0.03	0.5
1e	4.1±5.2	-	-
1f	>100	-	-
1g	>100	-	-
1h	>100	-	-
1i	>100	-	-
1j	70.4±29	-	-
2a	50.3±26	-	-
2b	0.056±0.09	37.3±24	666
2c	7.4±5.6	32.1±21	4
2d	11.0±1.7	68.7±4	6
3a	22.5±22	-	-
3b	0.53±0.8	64.6±31	121

[a] IC_{50} values were calculated as the concentration of compound required for 50% cell viability inhibition as estimated by GraphPad Prism software. Values are the mean±SD of at least three independent experiments.

[b] SI: IC_{50}HEK293/IC_{50}MCF-7.

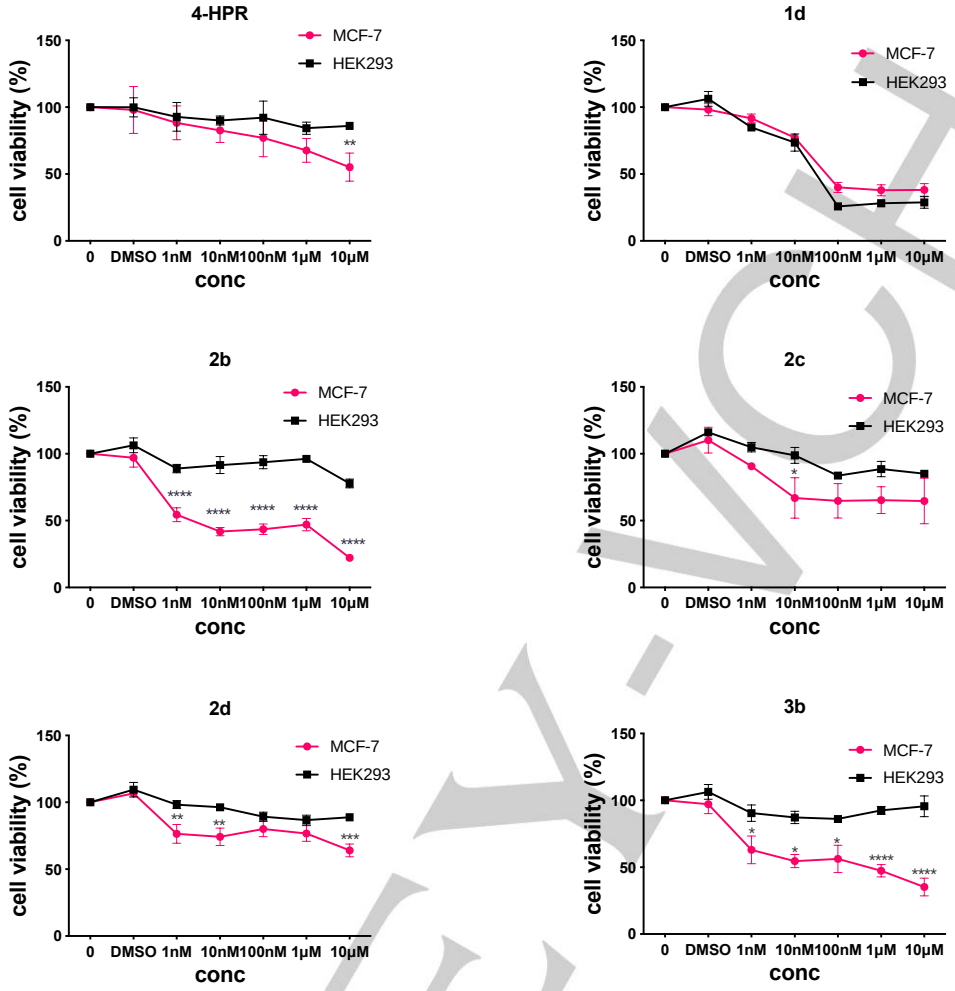

Figure 3. Cell viability curves of MCF-7 or HEK293 cells after treatment with 4-HPR and compounds **1d**, **2b**, **2c**, **2d** and **3b** at different concentrations. Untreated cells (0) or VEH cells (DMSO) were used as negative control. Each data point is the mean±SEM of three independent experiments performed in triplicate. Significance *P<0.05, **P<0.01, ***P<0.001, ****P<0.0001 calculated by two-way ANOVA with Bonferroni post-hoc test.

***In vitro* characterisation of the anti-cancer mechanism of the lead compounds 2b and 3b.**

Compounds **2b** and **3b** – showing the most promising results in term of efficacy and selectivity – were therefore tested through signalling assays in order to characterize the biological pathways involved in their anticancer activity. Although the anti-cancer mechanism of 4-HPR is not yet completely elucidated, the most credited hypothesis is based on the capacity of 4-HPR to generate ROS which might induce apoptosis of cancer cells. Specifically, the pro-apoptotic activity induced by 4-HPR is mediated by the activation of mitogen-activated proteins serine/threonine kinases (MAPKs) such as JNKs, p38, ERK and PKC.[21] In addition, apoptosis is triggered by the Endoplasmic Reticulum (ER) stress which in turn is induced by ROS generation.[27] Also caspases play a role in 4-HPR-induced apoptosis and their activity can be assessed detecting the cleavage of Poly(ADP-Ribose) Polymerase 1 (PARP-1), which is a cellular substrate of caspases.[28] Therefore, these downstream signalling pathways were investigated in MCF-7 cells after 24 hours treatment with compounds **2b** and **3b**.

Interestingly, both **2b** and **3b** – as 4-HPR – induced PARP-1 cleavage in MCF-7 cells when compared to the untreated (0) or vehicle control (DMSO), confirming the involvement of caspases in their apoptotic mechanism (Figure 4A, panel 1). Furthermore, the capacity of selected compounds to induce apoptosis via ER stress was evaluated through western blot analyses of the immunoglobulin Binding Protein (BiP) GRP-78. The synthesis of BiP is markedly induced under stress conditions leading to the accumulation of unfolded polypeptides in the ER, which in particular circumstances promotes the cells apoptotic death via the Unfolded Protein Response (UPR) signalling network.[29] Interestingly, we observed that BiP was significantly increased in MCF-7 cells after treatment with concentrations ≥ 5 μM of compound **2b**, as well as with 4-HPR. Conversely, compound **3b** was capable to significantly increase BiP only at 10 μM concentration (Figure 4A, panel 2, 4B). Finally, we observed compound **2b** to significantly induce p38 phosphorylation at concentrations ≥ 5 μM, while no significant increase was observed in cells treated with **3b** (Figure 4A, panel 3, 4C).

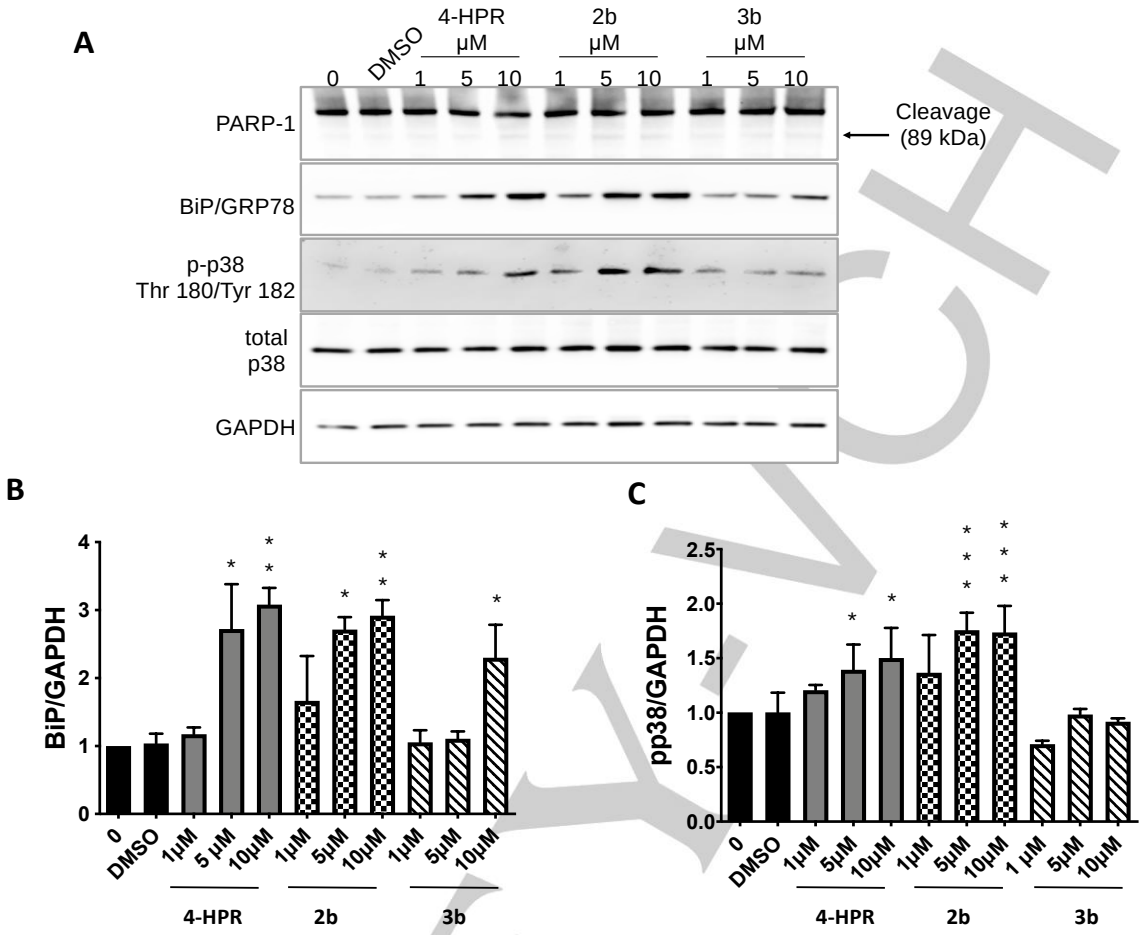

Figure 4. A) Western blot analyses of PARP-1 cleavage, BiP/GRP-78 and pp38 in MCF-7 cells treated with 4-HPR or **2b** or **3b** at different concentrations of 1, 5 and 10 μM. Untreated cells (0) and VEH cells (DMSO) were used as negative control. Protein levels of GAPDH were used as confirmation of equal loading of samples. Representative images are shown. B) Graphical representation of BiP/GAPDH. C) Graphical representation of pp38/GAPDH. Data are normalised to GAPDH and are the mean±SEM of three independent results. Significance calculated by one-way ANOVA with Dunnett's multiple comparison test. *P<0.05, **P<0.01, ***P <0.001 vs 0 or DMSO.

Studies on 3T3-L1 adipocytes to evaluate the anti-obesity/diabetic properties

In addition to its anti-cancer role, 4-HPR has been suggested to exhibit anti-obesity/diabetic properties. Previous studies have attributed these properties to the ability of 4-HPR to inhibit adipogenesis via an ATRA-dependent mechanism by activation of ATRA receptors (RAR) and genes involved in retinoids metabolism.[7] However, it is also known that 4-HPR acts via different ATRA independent pathways. For example, 4-HPR – unlike ATRA[30] – can inhibit the enzyme Desaturase1 (Des1).[1,31] This enzyme is able to catalyse the final step in the *de novo* Cer biosynthesis, introducing a double bond in dihydroceramide (dhCer) to form Cer.[8] Interestingly, the Des1 gene has been identified as a hot spot in a genome-wide association study of obesity traits and excessive amount of Cer might be responsible for lipotoxicity.[32] Furthermore, accumulation of Cer is responsible for inducing the activation of phosphatase 2A which in turn promotes the dephosphorylation of Akt/PKB. Importantly, activation of the Akt pathway is involved in glucose homeostasis and insulin signalling, promoting the translocation of the glucose transporter to the plasma membrane and hereby enabling glucose uptake from the bloodstream.[7] We sought therefore to investigate if these pathways could also be involved in the mechanism of action of our novel compounds.

The potential anti-obesogenic activity was assessed by testing the capacity of compounds **1a-j**, **2a-d** and **3a-b** to reduce the amount of lipid accumulation in 3T3-L1 adipocytes during differentiation using the Oil Red O stain. We observed that both 4-HPR and ATRA significantly inhibited adipogenesis, as previously reported[7] (Figure 5A-B). However, treatment with most of the newly synthesised analogues did not reduce the accumulation of lipids in 3T3-L1 adipocytes. Interestingly, we found a significant decrease in lipid accumulation only when 3T3-L1 adipocytes were treated with compounds **1d, 2b** and **2d** but to a lesser degree if compared to 4-HPR and ATRA. Although the reduced lipid accumulation observed for **1d** was presumably ascribed to its unspecific cytotoxicity, the anti-adipogenesis effect of **2b** and **2d** might be correlated with the presence of the characteristic 4-HPR phenol ring in both structures. Importantly, we observed that also the click-type analogue **3b** was able to significantly reduce lipid accumulation although to a lesser extent if compared to 4-HPR and ATRA (Figure 5A-B).

Our results suggest that modifications on the 4-HPR's scaffold might affect the interactions with the RAR signalling pathway, thus decreasing the anti-adipogenesis activity of the new analogues.

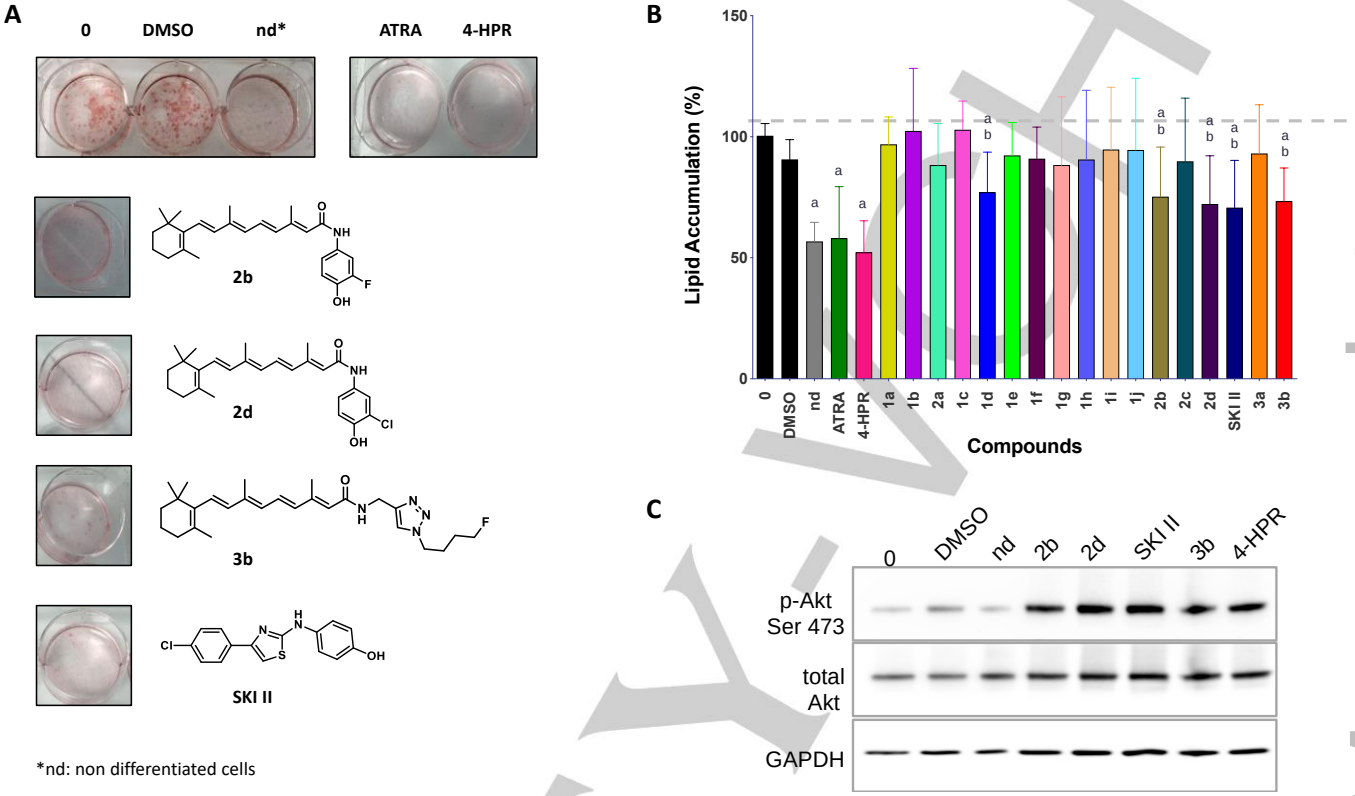

Figure 5. A) Images of lipid stained with Oil Red O and B) quantification of the absorbance at 520 nm after treatment of 3T3-L1 adipocytes during differentiation with ATRA, 4-HPR, SKI II and compounds **1a-j**, **2a-d** and **3a-b.** Data are the average of three independent results. Significance calculated by one-way ANOVA with Dunnett's multiple comparison test. a = P < 0.05 vs 0 or DMSO, b = P < 0.05 vs 4-HPR. C) Representative images of western blot analyses of p-Akt in 3T3-L1 adipocytes after treatment with 4-HPR, SKI II and compounds **2b**, **2d** and **3b.** Untreated cells (0) and VEH cells (DMSO) were used as negative control. Protein levels of GAPDH were used as confirmation of equal loading of samples.

In order to investigate whether the decrease in lipid accumulation was also correlated with Des1 inhibition, the Des1 inhibitor SKI II was screened. We observed that SKI II slightly inhibited adipogenesis compared with 4-HPR (Figure 5A-B). SKI II has been reported to be a more potent Des1 inhibitor (K_i = 0.3 μM)[33,34] than 4-HPR (K_i = 8 μM)[31], therefore we concluded that the mechanism utilised by 4-HPR – and presumably by compounds **2b**, **2d** and **3b** – in reducing lipid accumulation might be due to a combined involvement of the ATRA-dependent and -independent pathways.

Furthermore, we also measured the increase of phospho-Akt/PKB (p-Akt) in 3T3-L1 cells during differentiation (Figure 5C). Western blotting for p-Akt determined a comparable increase in p-Akt and suggested a comparable activity of compounds **2b**, **2d** and **3b** with 4-HPR (Figure 5C), thus reflecting the results obtained with the Oil Red O stain. Therefore, the regulation of this downstream signalling pathway represents a promising target to prevent insulin resistance and type-2 diabetes.

RADIOCHEMISTRY

Radiosynthesis of [^{18}F]3b

Based on the positive *in vitro* results, compound **3b** was developed as a PET tracer. Importantly, the CuAAC using a fluorine-18 labeled azide is a common approach for the radiolabeling of bioactive molecules which – as in our case – lack stability under conventional radiofluorination reaction conditions (especially pH and temperature).[35] Our strategy consisted of reacting the radiolabeled azide [^{18}F]**5** – obtained in turn from precursor **4** and K[^{18}F]F-K_{222} at high temperature – with the sensitive alkyne **1k** (Scheme 3). [^{18}F]**5** was reacted with **1k** either after purification via distillation or directly in a one-pot strategy. Although we observed the formation of the product [^{18}F]**3b** using both strategies, the purification of the one-pot mixture was quite challenging and no pure [^{18}F]**3b** could be obtained. Conversely, the purification of the tracer [^{18}F]**3b** was possible using HPLC, when the azide [^{18}F]**5** was distilled. This resulted in [^{18}F]**3b** with a satisfactory UV purity, a radiochemical purity of 95% immediately after purification and a radiochemical yield of 17% (decay corrected). A progressive degradation of the tracer was observed over time in HPLC eluent and the degradation was even faster in the formulation buffer. After HPLC purification the tracer was collected in a mixture containing a reduced percentage of water, while in the formulation buffer the organic solvent was reduced to 10%, therefore we ascribed the fast degradation of the tracer

during this stage to a low stability in water. Since the degradation process of the corresponding non-radioactive compound was much slower – an aqueous solution of [^{19}F]**3b** was stable for several days in similar conditions – we attributed this fast decomposition to radiolysis of water and subsequent ROS generation which may be responsible for the degradation of the tracer [^{18}F]**3b**. The addition of anti-oxidant stabilizers was also tested, but the stability of the tracer was not improved. Radiolytic decomposition is a common issue in radiopharmaceuticals development – mostly when the product is prepared in high doses – and considerable efforts are required to limit this phenomenon.[36] There is evidence in literature that the structural characteristics of the tracer as well as the ingredients present in the aqueous solution can affect the stability of PET tracer formulations.[37–42] Several factors should be therefore considered when a new PET tracer is formulated. This was also confirmed by our experience and further attempts are warranted to improve the stability of [^{18}F]**3b**.

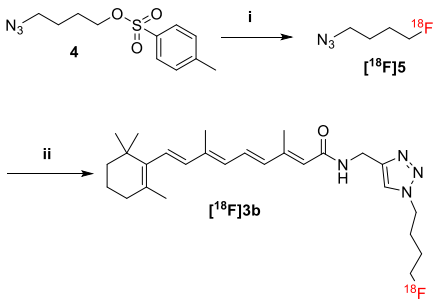

Scheme 3. Radiosynthesis of [^{18}F]**3b**. Reagents and conditions: i) K[^{18}F]F-K_{222}, DMF, 90 °C, 10 min; ii) **1k**, $CuSO_4$, sodium ascorbate, DMF/H_2O, 35 °C, 15 min.

Conclusion

In the present study, a library of 4-HPR analogues was synthesised by using a single step amide coupling (**1a-j** and **2a-d**) or through CuAAC (**3a-b**). Subsequently, these compounds were evaluated *in vitro* to assess their anti-cancer activity and their capacity to potentially prevent metabolic syndrome. Our results indicated that certain modifications on the 4-HPR scaffold, specifically on the aromatic ring (**1d**, **2b** and **3b**), improved the capacity to inhibit MCF-7 cells viability as well as their selectivity (**2b** and **3b**). Taken together, our preliminary results suggest that **2b** and **3b** might represent promising anti-cancer agents to be tested *in vivo*. The *in vivo* chemotherapeutic activity of 4-HPR is compromised by its low bioavailability which results in insufficient concentrations of drug in the blood – as well as in cancer tissues – which would be required to induce apoptosis of cancer cells. Since compounds **2b** and **3b** are more potent in the inhibition of cancer cell viability *in vitro*, even low concentrations might be sufficient to promote the same effect in cancer tissues *in vivo*. On the other hand, 4-HPR analogues with improved anti-adipogenesis activity in 3T3-L1 adipocytes – relative to ATRA and 4-HPR – could not be identified. Finally, we successfully radiosynthesised [^{18}F]**3b** as a candidate PET imaging tracer. Although we could not use [^{18}F]**3b** in pre-clinical PET imaging studies, owing to its insufficient chemical stability, we showed that the non-radioactive click-type derivative **3b** has interesting biological properties. We observed that the introduction of the 1,2,3-triazole group increases the hydrophilicity of **3b** (calculated LogP = 5.34-5.89 vs. experimental LogP = 6.31 for 4-HPR,[43] see Supporting Information for more details) without dramatically affecting the *in vitro* behaviour, as confirmed by our preliminary *in vitro* results. Importantly, the low bioavailability of 4-HPR is mostly related to the hydrophobic nature of the molecule. Hence, the more hydrophilic derivative **3b** may represent a valid alternative for developing 4-HPR derivatives with increased hydrophilicity and improved bioavailability.

Experimental Section

General Information

Dry solvents were obtained from commercial sources and used without further purification. Reactions performed under nitrogen atmosphere were carried out in dry solvents. Reactions were monitored by thin-layer chromatography (TLC), unless otherwise noted. TLCs were performed on Merck silica gel glass plates (60 F254). Visualisation was accomplished by UV light (254 nm) or staining with ceric ammonium molybdate or $KMnO_4$ solution. Flash chromatography (FC) was performed manually using Silica gel (60 Å, particle size 40–63 µm) purchased from Merck. Lab handling of the molecules was performed in dim light and using vessels wrapped with aluminium foil. ^{1}H NMR and ^{13}C NMR spectra were recorded on a Bruker AVANCE III 400 NMR spectrometer and calibrated using residual undeuterated solvent as internal reference. ^{19}F NMR spectra were recorded on a Bruker AVANCE III 400 NMR spectrometer and were referenced to $CFCl_3$. ^{13}C NMR spectra were recorded with complete proton decoupling. Chemical shifts (δ) are reported in parts per million (ppm) and coupling constants (J) are given in Hertz (Hz), multiplicity is described using the following abbreviations: s = singlet, d = doublet, t = triplet, q = quartet, m = multiplet, br = broad, or combinations thereof. Mass analyses were performed using Agilent 1200 HPLC system coupled to Agilent G6120 single quadrupole detector equipped with an electrospray ionization (ESI) source in direct infusion modality. ESI-MS spectra were recorded in positive mode. RP-HPLC-MS analyses were performed with an Agilent 1200 HPLC system equipped with a DAD and an ESI-MS detector. HPLC conditions for analytical analyses: Phenomenex Luna C18 column, 5 µm, 100 Å, 250 × 4.6 mm (L × ID) injected volume 10 µL, flow rate 1 mL/min, unless otherwise specified. HPLC preparative purification was performed using an Agilent 1260 HPLC system equipped with DAD detector, HPLC conditions for preparative purification: Phenomenex Luna C18 column, 5 µm, 100 Å, 250 × 21.2 mm (L × ID), flow rate 20 mL/min. Radioactivity levels were measured using a Veenstra VDC-405 dose calibrator. Radiochemistry was carried out in house assembled remotely controlled device.[44] RP-HPLC analyses of the radiotracer and precursors were performed using a Shimadzu SPD-20A system equipped with a PDA UV detector and HERM LB500 activity detector and LabSolutions 5.85 software (Shimadzu Corporation, Japan). HPLC semi-preparative purification of the radiotracer was performed using Jasco (Jasco Benelux, de Meern, the Netherlands) HPLC system.

General procedure for the synthesis of compounds 1a-k and 2a-d (General procedure A)

To a stirred solution of ATRA (1.0 equiv,100.0 mg, 0.33 mmol), HATU (1.5 equiv, 188.2 mg, 0.49 mmol) and DIPEA (3.0 equiv, 0.17 mL, 0.99 mmol) or 2,4,6-collidine (3.0 equiv, 0.13 mL, 0.99 mmol) in DCM (4 mL), the appropriate benzylamine or aniline (1.5 equiv, 0.49 mmol) was added. The mixture was stirred overnight at room temperature under nitrogen atmosphere. The reaction was quenched with saturated NH_4Cl (10 mL), extracted with DCM (3x30 mL), washed with brine (10 mL), dried over Na_2SO_4 and concentrated under vacuum at low temperature. After a first purification by FC, the compounds synthesised were subjected to RP-HPLC analyses and then, depending on the HPLC profile and separation,

a further preparative RP-HPLC purification was required in order to achieve a higher degree of purity.

(2E,4E,6E,8E)-*N*-(4-fluorophenyl)-3,7dimethyl-9-(2,6,6-trimethylcyclohex-1-en-1yl)nona-2,4,6,8-tetraenamide (1a)

ATRA was reacted with 4-fluoro-aniline (55.0 mg, 0.49 mmol), HATU and DIPEA according to general procedure **A**. The crude was purified by FC using *n*-Hex/EtOAc (8:2) to obtain **1a** in 60% yield (78.0 mg) as a yellow solid. R_f = 0.5 (*n*-Hex/EtOAc 9:1). Analytical RP-HPLC: solvent A: H_2O, solvent B: MeOH, gradient from 90% to 95% of B in 30 min, rt = 14.9 min. MS (ESI, m/z): $C_{26}H_{33}FNO$ $[M+H]^+$ calc. 394.25, found 394.3, $C_{26}H_{32}FNNaO$ $[M+Na]^+$ calc. 416.25, found 416.3. ^{1}H NMR ($CDCl_3$, 400 MHz), *δ*: 7.53 (br, 2H), 7.42 (br,1H), 7.04-6.97 (m, 3H), 6.32-6.14 (m, 4H), 5.82 (s, 1H), 2.43 (s, 3H), 2.06-2.02 (m, 5H), 1.74 (s, 3H), 1.66-1.62 (m, 2H), 1.51-1.48 (m, 2H), 1.06 (s, 6H). ^{19}F NMR ($CDCl_3$, 376 MHz), *δ*: -119.64 (m, 1F). ^{13}C NMR ($CDCl_3$, 101 MHz), *δ*: 165.2, 159.2 (d, J_{C-F} = 244.8 Hz), 150.8, 139.4, 137.7, 137.3, 135.2, 134.3, 130.6, 130.0, 129.5, 128.6, 121.5 (d, J_{C-F} = 6.3 Hz), 121.0, 115.6 (d, J_{C-F} = 22.2 Hz), 39.6, 34.3, 33.1, 29.0, 21.8, 19.2, 13.7, 12.9.

(2E,4E,6E,8E)-*N*-(3-trifluoromethyl-phenyl)-3,7dimethyl-9-(2,6,6-trimethylcyclohex-1-en-1yl)nona-2,4,6,8-tetraenamide (1b)

ATRA was reacted with 3-trifluoromethyl aniline (80.0 mg, 0.49 mmol), HATU and DIPEA according to general procedure **A**. The crude was purified by FC using *n*-Hex/EtOAc (9:1) to obtain **1b** in 67% yield as an orange solid (90.0 mg). R_f = 0.35 (*n*-Hex/EtOAc 9:1). Analytical RP-HPLC: solvent A: H_2O, solvent B: CH_3CN, gradient from 87% to 100% of B in 15 min, then 100% of B, rt = 16.04 min. MS (ESI, m/z): $C_{27}H_{33}F_3NO$ $[M+H]^+$ calc. 444.24, found 444.3. ^{1}H NMR ($CDCl_3$, 400 MHz), *δ*: 7.90 (br, 1H), 7.76 (d, *J* = 8.0 Hz, 1H), 7.63 (br, 1H), 7.44 – 7.31 (m, 2H), 7.03 (dd, *J* = 15.0, 11.5 Hz, 1H), 6.35 – 6.12 (m, 4H), 5.83 (s, 1H), 2.45 (s, 3H), 2.09 – 1.99 (m, 5H), 1.74 (s, 3H), 1.67-1.61 (m, 2H), 1.51-1.48 (m, 2H), 1.06 (s, 6H). ^{19}F NMR ($CDCl_3$, 376 MHz) *δ*: -62.72 (m, 3F). ^{13}C NMR ($CDCl_3$, 101 MHz), *δ*: 165.5, 151.7, 139.7, 138.9, 137.7, 137.2, 135.0, 131.3 (q, J_{C-F} = 29.2Hz), 131.0, 130.1, 129.4, 128.8, 123.9 (q, J_{C-F} = 273.3 Hz), 122.8, 120.56, 120.49, 120.45, 39.6, 34.3, 33.1, 29.0, 21.8, 19.2, 13.8, 12.9.

(2E,4E,6E,8E)-*N*-(3-*tert*-Butyl-phenyl)-3,7dimethyl-9-(2,6,6-trimethylcyclohex-1-en-1yl)nona-2,4,6,8-tetraenamide (1c)

ATRA was reacted with 3-(*t*-butyl)aniline (74.0 mg, 0.49 mmol), HATU and DIPEA according to general procedure **A**. The crude was purified by FC using *n*-Hex/EtOAc (9:1) to obtain **1c** in 63% yield as a yellow solid (90.0 mg). R_f = 0.4 (*n*-Hex/EtOAc 9:1). Analytical RP-HPLC: solvent A: H_2O, solvent B: CH_3CN, gradient from 93% to 100% of B in 15 min, then 100% of B, rt = 14.98 min. MS (ESI, m/z): $C_{30}H_{42}NO$ $[M+H]^+$ calc. 432.32, found 432.3. ^{1}H NMR ($CDCl_3$, 400 MHz) *δ*: 7.92 (s, 1H), 7.64 (br, 1H), 7.50 (d, *J* = 7.2 Hz, 1H), 7.25 (t, *J* = 7.2 Hz, 1H), 7.14 (d, *J* = 7.2 Hz, 1H), 6.99 (dd, J = 15.0, 11.4 Hz, 1H), 6.33 – 6.15 (m, 4H), 5.93 (s, 1H), 2.46 (s, 3H), 2.09–2.03 (m, 5H), 1.77 (s, 3H), 1.70-1.64 (m, 2H), 1.53-1.50 (m, 2H), 1.33 (s, 9H), 1.08 (s, 6H).^{13}C NMR ($CDCl_3$, 101 MHz) *δ*: 165.5, 152.1, 150.1, 139.0, 138.2, 137.8, 137.4, 135.6, 130.2, 129.9, 129.7, 128.6, 128.4 , 121.9, 121.1, 117.2, 117.0, 39.6, 34.7, 34.3, 33.1, 31.3, 29.0, 21.8, 19.3, 13.8, 12.9.

(2E,4E,6E,8E)-*N*-(diphenyl)-3,7dimethyl-9-(2,6,6-trimethylcyclohex-1-en-1yl)nona-2,4,6,8-tetraenamide (1d)

ATRA was reacted with 4-Aminobiphenyl (83.7 mg, 0.49 mmol), HATU and DIPEA according to general procedure **A**. The crude was purified by FC using *n*-Hex/EtOAc (9:1) to obtain **1d** in 60% yield as a white solid (89.0 mg). R_f = 0.5 (*n*-Hex/EtOAc 8:2). Analytical RP-HPLC: solvent A: H_2O, solvent B: CH_3CN, gradient from 93% to 100% of B in 15 min, then 100% of B, rt = 14.15 min. MS (ESI, m/z): $C_{32}H_{38}NO$ $[M+H]^+$ calc. 452.29, found 452.3, $C_{32}H_{37}NNaO$ $[M+Na]^+$ calc. 474.29, found 474.2. ^{1}H NMR ($(CD_3)_2SO$, 400 MHz) *δ*: 10.11 (s, 1H), 7.76 (d, *J* = 8.7 Hz, 2H), 7.71 – 7.58 (m, 4H), 7.46-7.42 (m, 2H), 7.33 (tt, *J* = 1.2, 7.2 Hz, 1H), 7.03 (dd, J = 15.1, 11.4 Hz, 1H), 6.46 – 6.13 (m, 4H), 6.07 (s, 1H), 2.38 (s, 3H), 2.11 – 1.96 (m, 5H), 1.71 (s, 3H), 1.63-1.55 (m, 2H), 1.49-1.41 (m, 2H), 1.03 (s, 6H). ^{13}C ($(CD_3)_2SO$, 101 MHz) *δ*: 165.3, 149.1, 140.2, 138.8, 137.8, 136.4, 135.1, 130.6, 130.4, 129.9, 129.4, 128.0, 127.3, 126.7, 123.0, 119.8, 39.6 (under solvent signal), 34.3, 33.1, 29.3, 22.0, 19.2, 13.8, 13.1.

(2E,4E,6E,8E)-*N*-(4-chlorophenyl)-3,7dimethyl-9-(2,6,6-trimethylcyclohex-1-en-1yl)nona-2,4,6,8-tetraenamide (1e)

ATRA was reacted with 4-Chloroaniline (68.0 mg, 0.49 mmol), HATU and DIPEA according to general procedure **A**. The crude was purified by FC using *n*-Hex/EtOAc (9:1) to obtain **1e** in 65% yield (90.0 mg) as an orange solid. R_f = 0.6 (n-Hex/EtOAc 7:3). Analytical RP-HPLC: solvent A: H_2O, solvent B: CH_3CN, gradient from 95% to 100% of B in 15 min, rt = 12.68 min. MS (ESI, m/z): $C_{26}H_{33}ClNO$ calc. $[M+H]^+$ 410.22, found 410.2. ^{1}H NMR ($CDCl_3$, 400 MHz) *δ*: 7.43 (d, *J* = 8.3 Hz, 2H), 7.25 (br, 1H), 7.22 – 7.15 (m, 2H), 6.91 (dd, *J* = 14.99, 11.37 Hz, 1H), 6.23-6.16 (m, 2H), 6.11 – 6.04 (m, 2H), 5.71 (s, 1H), 2.34 (s, 3H), 2.01 – 1.89 (m, 5H), 1.65 (s, 3H), 1.58 – 1.51 (m, 2H), 1.44 – 1.37 (m, 2H), 0.96 (s, 6H).^{13}C NMR ($CDCl_3$, 101 MHz) *δ*: 165.1, 151.3, 139.6, 137.7, 137.2, 136.9, 135.1, 130.8, 130.0, 129.4, 129.0, 128.7, 120.9, 120.7, 39.6, 34.3, 33.1, 29.0, 21.8, 19.2, 13.8, 12.9.

(2E,4E,6E,8E)-*N*-(benzyl)-3,7dimethyl-9-(2,6,6-trimethylcyclohex-1-en-1yl)nona-2,4,6,8-tetraenamide (1f)

ATRA was reacted with benzylamine (53.8 mg, 0.49 mmol), HATU and DIPEA according to general procedure **A**. The crude was purified by FC using *n*-Hex/EtOAc (9:1). The product was then submitted to an additional preparative RP-HPLC purification: solvent A: H_2O, solvent B: CH_3CN, isocratic 93% B to obtain the final product **1f** as a yellow solid in 89% yield (117.0 mg). R_f = 0.35 (*n*-Hex/EtOAc 8:2). Analytical RP-HPLC: gradient from 93% to 100% of B in 20 min, rt = 9.86 min. MS (ESI, m/z): $C_{27}H_{36}NO$ $[M+H]^+$ calc. 390.27, found 390.3, $C_{27}H_{35}NNaO$ $[M+Na]^+$ calc. 412.27, found 412.2. ^{1}H NMR ($CDCl_3$, 400 MHz) *δ*: 7.37 – 7.29 (m, 5H), 6.95 (dd, *J* = 15.0, 11.4 Hz, 1H), 6.31 – 6.10 (m, 4H), 5.92 (t, *J* = 5.6 Hz, 1H), 5.71 (s, 1H), 4.50 (d, *J* = 5.6 Hz, 2H), 2.41 (s, 3H), 2.09 – 1.99 (m, 5H), 1.74 (s, 3H), 1.69 – 1.60 (m, 2H), 1.53 – 1.47 (m, 2H), 1.06 (s, 6H). ^{13}C NMR ($CDCl_3$, 101 MHz) *δ*: 166.9, 149.0, 138.8, 138.6, 137.8, 137.4, 135.6, 129.84, 129.81, 128.7, 128.2, 127.8, 127.4, 121.2, 43.4, 39.6, 34.3, 33.1, 29.0, 21.8, 19.3, 13.7, 12.9.

(2E,4E,6E,8E)-*N*-(3-chlorophenyl)-3,7dimethyl-9-(2,6,6-trimethylcyclohex-1-en-1yl)nona-2,4,6,8-tetraenamide (1g)

ATRA was reacted with 3-chloroaniline (68.0 mg, 0.49 mmol), HATU and DIPEA according to general procedure **A**. The crude was purified by FC using *n*-Hex/EtOAc (9:1) and then submitted to an additional preparative RP-HPLC purification: solvent A: H_2O, solvent B: CH_3CN from 96% to 100% of B in 12 min. The final product **1g** was obtained as a yellow solid in 70% yield (130.0 mg). R_f = 0.6 (*n*-Hex/EtOAc 8:2). Analytical RP-HPLC: gradient from 96% to 100% of B in 12 min, rt = 10.51 min. MS (ESI, m/z): $C_{26}H_{33}ClNO$ calc. $[M+H]^+$ 410.22, , found 410.2. ^{1}H NMR ($CDCl_3$, 400 MHz) *δ*: 7.70 (br, 1H), 7.42 (br, 1H), 7.37 (d, *J* = 8.0 Hz, 1H), 7.20 (t, *J* = 8.0 Hz, 1H), 7.06 – 6.94 (m, 2H), 6.31 – 6.10 (m, 4H), 5.78 (s, 1H), 2.41 (s, 3H), 2.05 – 1.97 (m, 5H), 1.71 (s, 3H), 1.65 – 1.57 (m, 2H), 1.48-1.45 (m, 2H), 1.02 (s, 6H). ^{13}C NMR ($CDCl_3$, 101 MHz) *δ*: 165.6, 151.4, 139.6, 139.6, 137.8, 137.3, 135.2, 134.6, 130.8, 130.1, 129.9, 129.6, 128.7, 124.0, 120.9, 119.9, 117.9, 39.7, 34.3, 33.2, 29.0, 21.8, 19.3, 13.8, 13.0.

(2E,4E,6E,8E)-*N*-(2,4-dichlorobenzyl)-3,7dimethyl-9-(2,6,6-trimethylcyclohex-1-en-1yl)nona-2,4,6,8-tetraenamide (1h)

ATRA was reacted with 2,4-chlorobenzylamine (87.0 mg, 0.49 mmol), HATU and DIPEA according to general procedure **A**. The crude was

purified by FC using *n*-Hex/EtOAc (9:1) to obtain the final product **1h** as a yellow solid in 88% yield (135.0 mg). R_f = 0.4 (*n*-Hex/EtOAc 9:1). Analytical RP-HPLC: solvent A: H_2O, solvent B: CH_3CN, gradient from 96% to 100% of B in 12 min, rt = 10.70 min. MS (ESI, m/z): $C_{27}H_{34}Cl_2NO$ $[M+H]^+$ calc. 458.19, found 458.3. ^1H NMR ($CDCl_3$, 400 MHz) *δ*: 7.34 (d, *J* = 2.0 Hz, 1H), 7.30 (d, *J* = 8.0 Hz, 1H), 7.17 (dd, *J* = 8.0, 2.0 Hz, 1H), 6.90 (dd, *J* = 15.0, 11.4 Hz, 1H), 6.29 – 6.09 (m, 5H), 5.70 (s, 1H), 4.48 (d, *J* = 6.1 Hz, 2H), 2.33 (s, 3H), 2.03 – 1.98 (m, 5H), 1.71 (s, 3H), 1.64 – 1.58 (m, 2H), 1.47 – 1.44 (m, 2H), 1.02 (s, 6H). ^{13}C NMR ($CDCl_3$, 101 MHz) *δ*: 167.1, 149.5, 139.0, 137.7, 137.3, 135.4, 134.7, 134.1, 133.8, 130.8, 130.1, 129.9, 129.5, 129.2, 128.4, 127.3, 120.7, 40.7, 39.6, 34.3, 33.1, 29.0, 21.8, 19.2, 13.7, 12.9.

(2E,4E,6E,8E)-*N*-(4-nitrophenyl)-3,7dimethyl-9-(2,6,6-trimethylcyclohex-1-en-1yl)nona-2,4,6,8-tetraenamide (1i)

ATRA was reacted with 4-nitroaniline (70.0 mg, 0.49 mmol), HATU and DIPEA according to general procedure **A**. The crude was purified by FC using *n*-Hex/EtOAc (9:1) to obtain the final product **1i** as an orange solid in 50% yield (70.0 mg). R_f = 0.5 (*n*-Hex/EtOAc 8:2). Analytical RP-HPLC: solvent A: H_2O, solvent B: CH_3CN, gradient from 96% to 100% of B in 15 min, rt = 9.55 min. MS (ESI, m/z): $C_{26}H_{33}N_2O_3$ $[M+H]^+$ calc.421.24, found 421.3. ^1H NMR ($CDCl_3$, 400 MHz) *δ*: 8.19 (d, *J* = 9.2 Hz, 2H), 7.75 (d, *J* = 9.2 Hz, 2H), 7.70 (s, 1H), 7.05 (dd, *J* = 15.0, 11.4 Hz, 1H), 6.33 – 6.13 (m, 4H), 5.82 (s, 1H), 2.44 (s, 3H), 2.04 – 2.00 (m, 5H), 1.72 (s, 3H), 1.65 – 1.60 (m, 2H), 1.49 – 1.46 (m, 2H), 1.03 (s, 6H). ^{13}C NMR ($CDCl_3$, 101 MHz) *δ*: 165.2, 153.2, 144.5, 143.1, 140.3, 137.7, 137.1, 134.7, 131.7, 130.2, 129.3, 129.1, 125.1, 119.9, 118.8, 39.6, 34.3, 33.1, 29.0, 21.8, 19.2, 13.9, 13.0.

(2E,4E,6E,8E)-*N*-(2-methoxyphenyl)-3,7dimethyl-9-(2,6,6-trimethylcyclohex-1-en-1yl)nona-2,4,6,8-tetraenamide (1j)

ATRA was reacted with o-Anisidine (62.5 mg, 0.49 mmol), HATU and DIPEA according to general procedure **A**. The crude was purified by FC using *n*-Hex/EtOAc (9:1) to obtain the final product **1j** as an orange solid in 85% yield (113.0 mg). R_f = 0.6 (*n*-Hex/EtOAc 8:2). Analytical RP-HPLC: solvent A: H_2O, solvent B: CH_3CN, gradient: from 96% to 100% of B in 15 min, rt = 10.48 min. MS (ESI, m/z): $C_{27}H_{36}NO_2$ $[M+H]^+$ calc.406.27, found 406.1, ^1H NMR ($CDCl_3$, 400 MHz) *δ*: 8.49 (br, 1H), 7.85 (br, 1H), 7.06 – 6.95 (m, 3H), 6.88 (dd, *J* = 8.0, 1.3 Hz, 1H), 6.34 – 6.14 (m, 4H), 5.88 (s, 1H), 3.70 (s, 3H), 2.44 (s, 3H), 2.06 – 2.03 (m, 5H), 1.75 (s, 1H), 1.68 – 1.60 (m, 2H), 1.52 – 1.47 (m, 2H), 1.06 (s, 6H). ^{13}C NMR ($CDCl_3$, 101 MHz) *δ*: 165.0, 150.2, 147.8, 139.1, 137.8, 137.4, 135.5, 130.2, 129.9, 129.6, 128.4, 128.1, 123.4, 121.9, 121.1, 119.6, 109.8, 55.7, 39.6, 34.3, 33.1, 29.1, 21.8, 19.2, 13.6, 12.9.

(2E,4E,6E,8E)-*N*-(propargyl)-3,7dimethyl-9-(2,6,6-trimethylcyclohex-1-en-1yl)nona-2,4,6,8-tetraenamide (1k)

ATRA was reacted with propargylamine (0.03 mL, 0.49 mmol), HATU and DIPEA according to general procedure **A**. The crude was purified by FC using *n*-Hex/EtOAc (8:2) to obtain **1k** as a yellow solid in 90% yield (100.0 mg). R_f = 0.5 (*n*-Hex/EtOAc 7:3). Analytical RP-HPLC: solvent A: H_2O, solvent B: CH_3CN, 85% of B isocratic, rt = 12.09. MS (ESI, m/z): $C_{23}H_{32}NO$ $[M+H]^+$ calc.338.24, found 338.2. ^1H NMR ($CDCl_3$, 400 MHz) *δ*: 6.92 (dd, *J* = 15.0, 11.5 Hz, 1H), 6.26 – 6.09 (m, 4H), 6.04 (br, 1H), 5.68 (s, 1H), 4.08 (dd, *J* = 4.9, 2.2 Hz, 2H), 2.35 (s, 3H), 2.21 (br, 1H), 1.99 (m, 5H), 1.69 (s, 3H), 1.61 – 1.58 (m, 2H), 1.46-1.43 (m, 2H), 1.01 (s, 6H). ^{13}C NMR ($CDCl_3$, 101 MHz) *δ*: 166.7, 149.6, 138.9, 137.7, 137.3, 135.4, 130.1, 129.8, 129.5, 128.3, 120.4, 79.9, 71.3, 39.6, 34.2, 33.1, 29.1, 28.9, 21.7, 19.2, 13.6, 12.8.

(2E,4E,6E,8E)-*N*-(4-hydroxybenzyl)-3,7dimethyl-9-(2,6,6-trimethylcyclohex-1-en-1yl)nona-2,4,6,8-tetraenamide (2a)

ATRA was reacted with 4-hydroxybenzylamine (61.0 mg, 0.49 mmol), HATU and 2,4,6-collidine according to general procedure **A**. The crude was purified by FC using *n*-Hex/EtOAc (7:3). The product was then submitted to an additional preparative RP-HPLC purification using solvent A: H_2O, solvent B: CH_3OH, gradient from 85% to 95% of B in 20 min to obtain the final product **2a** as a yellow solid in 60% yield (80.0 mg). R_f = 0.5 (*n*-Hex/EtOAc 5:5). Analytical RP HPLC: 85% to 95% of solvent B in 20 min, rt = 13.48. MS (ESI, m/z): $C_{27}H_{36}NO_2$ $[M+H]^+$ calc. 406.27, found 406.3. ^1H NMR ($CDCl_3$, 400 MHz) *δ*: 7.16 (d, *J* = 8.5 Hz, 2H), 6.93 (dd, *J* = 15.0, 11.3 Hz, 1H), 6.79 (d, *J* = 8.5 Hz, 2H), 6.24 – 6.10 (m, 4H), 5.70 (t, *J* = 5.6 Hz, 1H), 5.66 (s, 1H), 4.41 (d, *J* = 5.6 Hz, 2H), 2.38 (s, 3H), 2.03 – 1.99 (m, 5H), 1.64 (s, 3H), 1.64 - 1.58 (m, 2H), 1.48 – 1.45 (m, 2H), 1.02 (s, 6H). ^{13}C NMR ($CDCl_3$, 101 MHz) *δ*: 167.4, 155.8, 149.3, 139.0, 137.7, 137.3, 135.4, 130.1, 129.9, 129.6, 129.5, 129.2, 128.4, 121.0, 115.7, 43.2, 39.6, 34.3, 33.1, 29.0, 21.8, 19.2, 13.8, 12.9.

(2E,4E,6E,8E)-*N*-(3-fluoro-4-hydroxy-phenyl)-3,7dimethyl-9-(2,6,6-trimethylcyclohex-1-en-1yl)nona-2,4,6,8-tetraenamide (2b)

ATRA was reacted with 4-amino-2-Fluorophenol (63.5 mg, 0.49 mmol), HATU and 2,4,6-collidine according to general procedure **A**. The crude was purified by FC using *n*-Hex/EtOAc (8:2). The product was then submitted to an additional preparative RP-HPLC purification using: solvent A: H_2O, solvent B: CH_3CN, gradient from 93% to 100% of B in 8 min, then 100% of B to obtain the final product **2b** as a yellow solid in 60% yield (81.0 mg). R_f = 0.5 (*n*-Hex/EtOAc 7:3). Analytical RP-HPLC: 93% to 100% of B in 8 min, then 100% of B, rt = 7.36 min. MS (ESI, m/z): $C_{26}H_{33}FNO_2$ $[M+H]^+$ calc. 410.24, found 410.3. ^1H NMR (CD_3OD, 400 MHz) *δ*: 7.53 (dd, *J* = 13.1, 2.3 Hz, 1H), 7.16 – 6.98 (m, 2H), 6.92 – 6.81 (m, 1H), 6.26 (m, 4H), 5.96 (s, 1H), 2.39 (s, 3H), 2.07-2.02 (m, 5H), 1.73 (s, 3H), 1.57 – 1.44 (m, 2H), 1.52 – 1.49 (m, 2H), 1.05 (s, 6H). ^{19}F NMR (CD_3OD, 376 MHz) *δ*: -137.84 (m, 1F). ^{13}C NMR (CD_3OD, 101 MHz) *δ*: 166.1, 150.9 (d, $J_{C\text{-}F}$ = 240.0 Hz), 149.6, 141.0 (d, $J_{C\text{-}F}$ = 15.9 Hz), 138.5, 137.7, 137.6, 135.6, 131.2 (d, $J_{C\text{-}F}$ = 7.9 Hz), 129.8, 129.7, 129.2, 127.8, 121.4, 117.1, (d, $J_{C\text{-}F}$ = 3.6 Hz), 115.8 (d, $J_{C\text{-}F}$ = 3.2 Hz), 108.2 (d, $J_{C\text{-}F}$ = 23.70), 39.4, 33.8, 32.6, 28.0, 20.6, 18.9, 12.5, 11.0.

(2E,4E,6E,8E)-*N*-(2-methyl-4-hydroxy-phenyl)-3,7dimethyl-9-(2,6,6-trimethylcyclohex-1-en-1yl)nona-2,4,6,8-tetraenamide (2c)

ATRA was reacted with 4-amino-3-methylphenol (61.5 mg, 0.49 mmol), HATU and 2,4,6-collidine according to general procedure **A**. The crude was purified by FC using *n*-Hex/EtOAc (9:1) to obtain the final product **2c** as a yellow solid in 60% yield (80.00 mg). R_f = 0.5 (*n*-Hex/EtOAc 8:2). Analytical RP-HPLC: solvent A: H_2O, solvent B: CH_3CN, gradient from 93% to 100% of B in 8 min, then 100% of B, rt = 7.08 min. MS (ESI, m/z): $C_{27}H_{36}NO_2$ $[M+H]^+$ calc. 406.27, found 406.2. ^1H NMR ($(CD_3)_2SO$, 400 MHz) *δ*: 9.18 (s, 1H), 9.13 (s, 1H), 7.12 (d, *J* = 8.5 Hz, 1H), 6.95 (dd, J = 15.0, 11.5, 1H), 6.60 (d, *J* = 2.5 Hz, 1H), 6.53-6.56 (dd, *J* = 8.5, 2.5 Hz, 1H), 6.15-6.38 (m, 4H), 6.08 (s, 1H), 2.32 (s, 3H), 2.10 (s, 3H), 2.03-1.98 (m, 5H), 1.70 (s, 3H), 1.60 -1.56 (m, 2H), 1.46-1.44 (m,2H), 1.03 (s, 6H). ^{13}C NMR ($(CD_3)_2SO$, 400 MHz) *δ*: 165.2, 155.2, 147.6, 138.3, 137.8, 137.5, 136.6, 134.1, 130.6, 129.8, 128.3, 127.8, 127.1, 123.4, 121.3, 117.0, 112.9, 49.06, 34.3, 33.1, 29.3, 22.0, 19.2, 18.6, 13.7, 13.1.

(2E,4E,6E,8E)-*N*-(3-chloro-4-hydroxy-phenyl)-3,7dimethyl-9-(2,6,6-trimethylcyclohex-1-en-1yl)nona-2,4,6,8-tetraenamide (2d)

ATRA was reacted with 4-amino-2-chlorophenol (72.0 mg, 0.495), HATU and 2,4,6-collidine according to general procedure **A**. The crude was purified by FC using *n*-Hex/EtOAc (8:2). The product was then submitted to a further preparative RP-HPLC purification: solvent A: H_2O and solvent B: CH_3CN, gradient from 93% to 100% of B in 8 min to obtain the final product **2d** as a yellow solid in 62% yield (88.0 mg). R_f = 0.5 (n-Hex/EtOAc 7:3). Analytical RP-HPLC: 93% to 100% of B in 8 min then 100% of B, rt = 8.31 min. MS (ESI, m/z): $C_{26}H_{33}ClNO_2$ calc. $[M+H]^+$ 426.21, found 426.2. ^1H NMR (CD_3OD, 400 MHz) *δ*: 7.57 (d, *J* = 2.5 Hz, 1H), 7.17 (dd, *J* = 8.8, 2.5 Hz, 1H), 6.95 (dd, *J* = 15.0, 11.3 Hz, 1H), 6.76 (d, *J* = 8.8 Hz, 1H), 6.30

– 6.01 (m, 4H), 5.85 (s, 1H), 2.27 (s, 2H), 1.97 – 1.88 (m, 5H), 1.61 (s, 3H), 1.58 – 1.51 (m, 2H), 1.43 – 1.37 (m, 2H), 0.94 (s, 6H). ^{13}C NMR (CD_3OD, 101 MHz) *δ*: 166.2, 149.6, 149.4, 138.5, 137.7, 137.6, 135.6, 131.6, 129.8, 129.6, 129.2, 127.8, 121.5, 121.4, 120.0, 119.6, 116.0, 39.4, 33.8, 32.6, 28.0, 20.5, 18.9, 12.5, 11.4.

General procedure for the synthesis of compounds 3a and 3b (General procedure B)

Benzylazide or *n*-butylazide was added to a solution of **1k** (1 equiv) in a 0.08 M solution of *t*-BuOH/H_2O (2:1). Sodium ascorbate (0.3 equiv) and $CuSO_4$ (0.1 equiv) were added to the solution and the reaction was stirred at room temperature. After complete consumption of the starting material, the reaction was quenched with saturated NH_4Cl and the mixture was extracted with DCM or EtOAc (3x30mL). The organic phase was dried over Na_2SO_4, the solvent was removed under reduced pressure at low temperature and the crude was purified by FC using the indicate solvent.

(2E,4E,6E,8E)-*N*-((1-benzyl-1H-1,2,3-triazol-4-yl)methyl)-3,7-dimethyl-9-(2,6,6-trimethylcyclohex-1-en-1yl)nona-2,4,6,8-tetraenamide (3a)

NaN_3 (152.0 mg, 2.34 mmol, 2 equiv) was added to a solution of benzylbromide (0.14 mL, 1.2 mmol, 1 equiv) in THF (2.5 mL) and the reaction was stirred at 80 °C overnight. 10 mL of H_2O were added to the reaction and the mixture was extracted with Et_2O (3x30 mL), washed with brine (1x10 mL), dried over Na_2SO_4 and concentrated under vacuum to obtain benzylazide as a pale oil. This was directly submitted to the next step without further purification. Benzylazide (34.0 mg, 0.25 mmol) was reacted with **1k** (86.2 mg, 0.25 mmol) sodium ascorbate (10.0 mg, 0.05 mmol) and $CuSO_4$ (1.60 mg, 0.01 mmol) according to general procedure **B** (overnight stirring). The crude was purified by FC (DCM/CH_3OH 9.8:0.2) to obtain compound **3a** as a yellow powder in 80% yield (96.0 mg). R_f = 0.2 (DCM/CH_3OH 9.8:0.2). Analytical RP HPLC: solvent A: H_2O, solvent B: CH_3CN, gradient from 85% to 100% of solvent B in 12 min, rt = 9.78 min. MS (ESI, m/z): $C_{30}H_{39}N_4O$ $[M+H]^+$ calc. 471.30, found 471.3. ^{1}H NMR ($CDCl_3$, 400 MHz) *δ*: 7.43 (s, 1H), 7 28 – 7.26 (m, 3H), 7.19 – 7.16 (m, 2H), 6.83 (dd, *J* = 15, 11.5 Hz, 1H), 6.61 (t, *J* = 5.5 Hz, 1H), 6.19 – 6.02 (m,4H), 5.63 (s, 1H), 5.40 (s, 2H), 4.44 (d, *J* = 5.5 Hz, 2H), 2.26 (s, 3H), 1.95 – 1.90 (m, 5H), 1.63 (s, 3H), 1.55 – 1.53 (m, 2H), 1.40 – 1.37 (m, 2H), 0.95 (s, 6H). ^{13}C NMR ($CDCl_3$), 400 MHz *δ*: 167.1, 149.0, 145.4, 138.7, 137.7, 137.3, 135.5, 134.5, 129.8, 129.6, 129.1, 128.8, 128.2, 128.1, 122.3, 121.1, 54.2, 39.6, 34.6, 34.2, 33.1, 29.0, 21.7, 19.2, 13.6, 12.9.

(2E,4E,6E,8E)-*N*-((1-(4-fluorobutyl-1H-1,2,3-triazol-4-yl)methyl)-3,7-dimethyl-9-(2,6,6-trimethylcyclohex-1-en-1yl)nona-2,4,6,8-tetraenamide (3b)

NaN_3 (98.00 mg, 1.5 mmol) was added to a solution of 1-Bromo-4-fluorobutane (155.0 mg, 1.00 mmol) in DMF (0.5 mL) and the reaction was stirred overnight at room temperature. Et_2O (1 mL) and H_2O (1 mL) were added to the mixture and the organic layer was directly transferred to a suspension of the alkyne **1k** (168.0 mg, 0.5 mmol). The mixture was reacted with $CuSO_4$ (8.0 mg, 0.05 mmol) and sodium ascorbate (30.0 mg, 0.15 mmol) for 4 h according to general procedure **B**. The crude product was purified by FC (*n*-Hex/EtOAc 5:5) to obtain **3b** as a yellow solid in 90% yield (200.0 mg). R_f = 0.5 (*n*-Hex/EtOAc 3:7). Analytical RP-HPLC: solvent A: H_2O, solvent B: CH_3CN, 85% of solvent B isocratic, rt = 10.56 min. MS (ESI, m/z): $C_{27}H_{40}FN_4O$ $[M+H]^+$ calc. 455.31, found 455.3. ^{1}H NMR ($CDCl_3$, 400 MHz) *δ*: 7.59 (s, 1H), 7.14 (br, 1H), 6.86 (dd, *J* = 15.0, 12.0 Hz, 1H), 6.21 – 6.04 (m, 4H), 5.74 (s, 1H), 4.48 (d, *J* = 5.6 Hz, 2H), 4.40 (t, *J* = 5.6 Hz, 2H), 4.32 (t, *J* = 6.8 Hz, 2H), 2.30 (s, 3H), 2.00 – 1.93 (m, 7H), 1.68 – 1.62 (m, 5H), 1.56-1.55 (m, 2H), 1.42 – 1.41 (m, 2H), 0.97 (s, 6H). ^{19}F-NMR ($CDCl_3$, 376 MHz) *δ*: -218.96 (m, 1F). ^{13}C NMR ($CDCl_3$, 400 MHz) *δ*: 167.3, 148.8, 145.2, 138.6, 137.7, 137.3, 135.6, 129.74, 129.71, 129.6, 128.1, 122.5, 121.3, 83.1 (d, $J_{C\text{-}F}$ = 165.5 Hz), 49.8, 39.6, 34.6, 34.2, 33.0, 28.9, 27.2 (d, $J_{C\text{-}F}$ = 20.2 Hz), 26.4 (d, $J_{C\text{-}F}$ = 4.0 Hz), 21.7, 19.2, 13.6, 12.8.

4-azidobutyl-4-methylbenzensulfonate (4)

4-bromo-1-butanol (300.0 mg, 1.96 mmol, 1.0 equiv) was dissolved in DMF (2 mL) and reacted overnight with NaN_3 (380.0 mg, 5.88 mmol, 3.0 equiv) heating at 70 °C. The reaction mixture was diluted with 5 mL of H_2O and the azide was extracted with Et_2O (3x30 mL). The organic phase was washed with 20 mL of brine and dried over Na_2SO_4. The volume of the solvent was reduced using a flow of nitrogen and the residue was directly reacted with tosyl chloride (747.0 mg, 3.92 mmol, 2.0 equiv) and Et_3N (0.55 mL, 3.92 mmol, 2.0 equiv) in 5 mL of DCM overnight. The mixture was diluted with 5 mL of H_2O and the product extracted with DCM (3x30 mL). The organic phase was washed with brine (10 mL), dried over Na_2SO_4 and concentrated under vacuum. The crude was purified by FC using *n*-Hex/EtOAc (9:1) to obtain compound **4** as a clear oil in 50% yield (260.0 mg). R_f = 0.4 (*n*-Hex/EtOAc 8:2). Analytical RP solvent A = H_2O, solvent B = CH_3CN; 0-3 min 5% B, gradient from 5% to 90% of B until 20 min, 20-25 min 90% B, rt = 22.06 min. MS (ESI, m/z): $C_{11}H_{16}N_3O_3S$ $[M+H]^+$ calc. 270.08, found 270.1, $C_{11}H_{16}N_1O_3S$ $[M+H\text{-}N_2]^+$ calc. 242.09, found 242.1. ^{1}H NMR ($CDCl_3$, 400 MHz) *δ*: 7.78 (d, *J* = 8.0 MHz, 2 H), 7.35 (d, *J* = 8.0 Hz, 2 H), 4.05 (t, *J* = 6.0 Hz, 2 H), 3.25 (t, *J* = 6.8 Hz, 2H), 2.44 (s, 3H), 1.76-1.58 (m, 4H). Analytical and spectroscopic data were consistent with those reported in the literature.[45]

Radiosynthesis of [^{18}F]3b

[^{18}F]fluoride was produced by the ^{18}O(p,n)^{18}F nuclear reaction on an IBA Cyclone 18/18 cyclotron (IBA, Louvain-la-Neuve, Belgium) and obtained as aqueous [^{18}F]F^-. 10 GBq of [^{18}F]F^- was trapped on an ion-exchange cartridge (PS-HCO_3, Chromafix, ABX Radeberg, Germany) and eluted into a screw cap reaction vessel (vial 1) using 1 mL of a 10 mL solution containing 20.0 mg of K_2CO_3 and 130.0 mg of K_{222} dissolved in a mixture of CH_3CN and water (9:1). Solvent was evaporated under vacuum using a Helium stream (50 mL/min) and heating the vial at 90 °C. Next, the temperature was reduced to 60 °C and 500 µL of dry CH_3CN (x2) were added. The temperature was increased again to 90 °C and solvent was evaporated by azeotropic drying. After complete evaporation of the solvent, the temperature was increased to 110 °C for 1 min. Subsequently, vial 1 was cooled to room temperature and precursor **4** (6.0 mg, 22.3 µmol) – previously dissolved in 200 µL of DMF – was added. The reaction was stirred at 90 °C for 10 min resulting in intermediate [^{18}F]**5** which was reacted with the alkyne precursor **1k** either after purification via distillation (**Procedure 1**) or directly in a one-pot strategy (**Procedure 2**). **Procedure 1:** The temperature of vial 1 was increased to 140 °C, while vial 2 was cooled to -20 °C. [^{18}F]**5** was distilled under a stream of Helium (10 mL/min) and 5 GBq of [^{18}F]**5** was collected in vial 2 containing the alkyne precursor **1k** (5.00 mg, 14 µmol) dissolved in 100 µL DMF. A solution of $CuSO_4$ (10 mg, 62 µmol) in water (50 µL) and a solution of sodium ascorbate (30 mg, 180 µmol) in water (50 µL) were mixed and diluted with 100 µL of DMF. When the solution turned from black to yellow this was added to the reaction mixture in vial 2. The suspension was stirred for 15 min at 35 °C and diluted with 1.5 mL of semi-prep HPLC eluent. The mixture was filtered on hydrophilic PTFE 0.45 µm filter and injected into the semi-prep RP-HPLC column (Phenomenex Luna C18, 5 µm, 250 mm x 10 mm, 100 Å; flow rate: 4 mL/min) using 15% H_2O/ 85% CH_3CN. The fraction corresponding to the desired product (rt = 16.0 min) was collected from the HPLC, diluted with at least 60 mL of water to have less than 10% CH_3CN and loaded onto a Sep-Pak t-C18 plus cartridge pre-activated using 10 mL of EtOH and 10 mL of water. The tracer was trapped on the cartridge, the Sep-Pak rinsed with water (20 mL), followed by elution of the product using 1.5 mL EtOH. Eventually, the solution of the tracer was diluted with 13.5 mL of a solution of 0.9% NaCl in water (saline) to reduce the content of EtOH to 10%. Formulated product was obtained in 17% RCY with a radiochemical purity of 95% at the end of synthesis. The radiochemical purity of [^{18}F]**3b** was determined using the following conditions: solvent A: H_2O, solvent B: CH_3CN; isocratic 85% of B, HPLC Column Grace AlltimaTM, C18 5 µm, 250 mm x 4.6 mm (Alltech, The Netherlands), injected volume 10 µL, flow rate: 1mL/min. The retention time of [^{18}F]**3b** was 10.61 min. **Procedure 2:** Vial 1 was cooled to room temperature and the alkyne precursor **1k** (11.0 mg, 30.0 µmol) dissolved in 100 µL of DMF was added to the mixture containing [^{18}F]**5**. $CuSO_4$ and sodium ascorbate were added as reported in Procedure 1 and the suspension was stirred for

15 min at 35 °C. The mixture was purified and formulated using the conditions reported in Procedure 1 providing [^{18}F]**3b** with a radiochemical purity < 95% (5% RCY).

Cell culture

The cell lines utilised throughout the present study were: the human breast adenocarcinoma cell line MCF-7, the human embryonic kidney 293 cells (HEK293) and the mouse embryonic fibroblast 3T3-L1 pre-adipocyte cell line. All procedures with MCF-7, HEK293 and 3T3-L1 cell cultures, unless otherwise stated, were carried out within a Cell Guard ES class II biological safety cabinet (NuAire, MN, USA) where surfaces had been wiped down with a 1% (w/v) Virkon disinfectant (DuPont, Stevenage, UK) and then sprayed with a 70% (v/v) ethanol solution prior to commencing work. Cells were maintained in media consisting of Dulbecco's Modified Eagle's Medium (DMEM) containing 4.5 g/L glucose (PAA, Somerset, UK), 10% (v/v) fetal bovine serum (#16170, Gibco (part of Invitrogen/Life Technologies), Paisley, UK) and 1% (v/v) sodium pyruvate (Lonza, Basel, Switzerland), termed growth media. During periods of proliferation, cells had their media replaced every three days with fresh growth media which was pre-warmed to 37 °C. Cell lines were incubated and maintained in a HERAcell 150 incubator (Thermo Scientific, UK) with a humidified environment at 37 °C with a 5% CO_2 concentration. Before reaching complete confluency, cultures were passaged in order to seed new culture flasks/plates or freeze cells down for storage. To passage cells, growth media was completely removed and cells were washed once with sterile phosphate buffered saline (PBS) from Lonza, in order to remove any remaining media and serum. PBS was removed and a Trypsin-EDTA (PAA, Somerset, UK) solution was added to cell cultures which were subsequently incubated for 5 min. Flasks were then gently agitated in order to assist with detachment of cells. Once detached, cells were diluted with fresh growth media in order to inactivate the Trypsin-EDTA solution and seeded to new flasks or cell culture plates.

Drug preparation

Fenretinide (4-HPR, Cilag AG, Schaffhausen, Switzerland), All-*Trans* Retinoic Acid (ATRA, fluorochem, UK), SKI II (Abcam, UK) and all experimental compounds **1a-j**, **2a-d** and **3a-b** were dissolved in DMSO at a stock concentration of 10 mM and stored at -20 °C avoiding excessive exposure to light. Stock solutions of compounds were then diluted to give the desired final working concentration, as indicated for each individual experiment. As a control, equivalent volumes of DMSO were always given to separate cultures in order to determine any effect of the vehicle on the experiment being undertaken.

MTT Assay

In order to perform the MTT assay, MCF-7 or HEK293 cells were seeded in 24 well plates at a density of 50.000 cells per well, counted using a hemocytometer. After one day, cells were stimulated overnight with 4-HPR, ATRA or experimental compounds **1a-j**, **2a-d** and **3a-b** at concentrations of 1 nM, 10 nM, 100 nM, 1 µM and 10 µM. Three additional wells served as controls: an untreated, a DMSO control and a well containing media only to determine background. Following 24 h of incubation at 37 °C, 250 µL of media were removed from each well and 25 µL of 3-(4,5-Dimethylthiazol-2-yl)-2,5-Diphenyltetrazolium Bromide (MTT) solution (5 mg/mL) were added to the well yielding a final concentration of 0.5 mg/mL. Plates were incubated at 37 °C for 3 h to allow formation of insoluble formazan crystals. Subsequently, the media was removed and the crystals dissolved in 320 µL of DMSO. Plates were wrapped in foil and shaken for 15 min to fully dissolve the coloured MTT formazan. Each well was transferred to a 96 well plate in triplicate (100 µL per well) and the absorbance was read at OD = 590 nm on a Spectramax Plus384 spectrophotometer (Molecular Devices, CA, USA). Background absorbance was determined from the cell-free control well and subtracted from each value. To determine the inhibition of cell growth for each drug treatment, data were expressed as percentage of the untreated control cells. Data were analysed and curves fitted using GraphPad Prism 5.04 to determine the IC_{50} of each compound.

Differentiation of 3T3-L1 pre-adipocytes and treatment

In order to differentiate 3T3-L1 pre-adipocyte cultures into mature adipocytes, cells were seeded into 6 well plates and grown to 100% confluency whilst being maintained in growth DMEM media. Once confluency was reached, cell cultures were left for an additional 2 days in order to allow for growth arrest to occur. Growth media was removed and replaced with a differentiation "cocktail" media named MDI (3-isobutyl-1-methylxanthine (M), dexamethasone (D) and insulin (I)), while one well containing normal growth media was used as control and was indicated as non-differentiated (nd) cells. MDI media was comprised of DMEM containing 4.5 g/L glucose, 10% (v/v) fetal bovine serum (#16170, Gibco part of Invitrogen/Life Technologies), 1% (v/v) sodium pyruvate, 1 µM dexamethasone, 10 µg/mL human insulin solution and 0.5 mM 3-isobutyl-1- methylxanthine (all from Sigma-Aldrich, UK). 3T3-L1 cells were either untreated or stimulated with 1 µM concentration of 4-HPR, ATRA, SKI II or experimental compounds **1a-j**, **2a-d** and **3a-b** and incubated for 48 h at 37 °C. MDI media was then replaced with insulin maintenance media consisting of all the components of MDI media except for dexamethasone and 3-isobutyl-1-methylxanthine and cells were once again either treated or untreated and incubated at 37 °C. After 2 days media was replaced with fresh insulin maintenance media and cells were for the last time either treated or untreated and incubated for other 2 days. At this point 3T3-L1 cells were deemed to be fully differentiated into adipocytes, therefore they were either stained with Oil Red O or overnight serum starved in order to perform western blot.

Oil Red O stain

After 8 days of 3T3-L1 differentiation, media was removed and cells fixed in formalin (Sigma Aldrich, UK) for 30 min at room temperature. Formalin was then removed and cells were stained with Oil Red O solution previously prepared as follows: 60 mg of Oil Red O powder (Sigma Aldrich, UK) dissolved in 20 mL of propan-2-ol, diluted (60% v/v) with distilled H_2O (dH_2O) and filtered through 3MM chromatography paper (Whatman, Maidstone, UK). Oil Red O staining was carried out for 1 h at room temperature, after which the stain was removed and fixed cell cultures were washed with dH_2O. Stained cells were then covered with 2 mL dH_2O for visualisation and image acquisition. For quantification purposes, dH_2O was removed from cell cultures and plates were allowed to dry completely. Oil Red O was eluted from cells by adding 1 mL of propan-2-ol and incubating at room temperature for 10 min. 100 µL of sample were loaded in triplicate into a 96 well plate using isopropanol as the blank and the absorbance read at 520 nm on a Spectramax Plus384 spectrophotometer (Molecular Devices, CA, USA). Background readings from isopropanol only wells were subtracted from sample values. To determine the lipid accumulation, absorbance readings for each drug treatment were expressed as a percentage of the differentiated untreated control.

Western blotting

MCF-7 cells were grown to confluency in 6 well plates. MCF-7 cells were either untreated or treated for 24 h with 1, 5 or 10 µM of 4-HPR or compounds **2b** or **3b**. For 3T3-L1 cells, following 8 days differentiation and treatment with or without 1 µM of compounds as reported above, cells were serum starved overnight and proteins harvested on the next day. MCF-7 and 3T3-L1 cell cultures were scraped in radioimmunoprecipitation assay (RIPA) lysis buffer (10 mM Tris-HCl (pH 7.4), 150 mM NaCl, 5 mM EDTA (pH 8.0), 1 mM NaF, 0.1% (w/v) SDS, 1% (v/v) Triton X- 100, 1% (w/v) sodium deoxycholate). Sodium orthovanadate (Na_3VO_4 at 2 mM) and protease inhibitors (complete protease inhibitor cocktail from Roche, UK, 1 tablet dissolved in 2 mL H_2O per 50 mL lysis buffer), were freshly added to the RIPA lysis buffer prior to start the protein extraction procedure. Samples were kept on ice at all times during the protein extraction process. Protein samples were then centrifuged using a refrigerated bench top

micro-centrifuge at 10,000 rpm for 10 min at 4 °C to pellet insoluble material, the supernatant was collected into new 1.5 mL centrifuge tube. Protein concentrations of each sample were determined using the BCA assay (Thermo Scientific, UK), following the manufacturer's protocols. Samples were run in duplicate and were compared to bovine serum albumin (BSA) protein standards ranging from 0.125 mg/mL to 2 mg/mL along with a RIPA blank set as 0 mg/mL. Protein lysates were combined with a 5X SDS sample buffer (250 mM Tris-HCl (pH 6.8), 10% (w/v) SDS, 50% glycerol, 0.025% (w/v) bromophenol blue and 5% (v/v) 2-mercaptoethanol) and RIPA buffer to give each sample the same final protein concentration. Typically, protein concentrations of 0.5-2 mg/mL were made for samples to be used for SDS-PAGE. SDS protein samples were then denatured by heating samples at 95 °C for 5 min and were then briefly centrifuged. SDS protein samples were stored at -20 °C until required. Samples were separated on 4-12% NuPAGE Bis-Tris (Invitrogen) gels by SDS-PAGE and transferred to 0.45 µm nitrocellulose membranes (BioRad, UK) in order to perform immunoblotting. Membranes were blocked for 1 h at room temperature with gentle agitation in TBS-T containing 5% (w/v) skimmed milk powder, cut for the protein of interest and then incubated overnight at 4 °C with primary antibodies: phospho-p38 MAPK (Thr180/Tyr182), total p38, PARP, BiP/GRP78, phospho-Akt/PKB (Ser 473) all from Cell Signalling, total Akt from Santa Cruz and GAPDH (ThermoFisher) was used as protein loading control. Primary antibodies were diluted 1:1000 in TBS-T with 5% (w/v) skimmed milk powder and then washed with TBS-T for 1-1.5 h changing solution every 15-20 min. Membranes were then incubated with secondary antibodies (goat anti-rabbit HRP-conjugated secondary antibody from Anaspec) diluted 1:5000 in TBS-T and 5% (w/v) skimmed milk powder at room temperature for 1 h. Membranes were washed once again in TBS-T for 1-1.5 h changing solution every 15-20 min. The enhanced chemiluminescence (ECL) reagent made in house (Reagent A: 100 mM Tris base pH 8.5, 2.5 mM Luminol and 0.4 mM p-Coumaric acid, Reagent B: 100 mM Tris base pH 8.5 and 0.06% (v/v) of 30% H_2O_2) was then applied to membranes for 1 min which were then dried of excess fluid. Membranes were exposed using the Fusion CCD camera (Peqlab, Sarisbury Green, UK) and then images were quantified using Image J software.

Acknowledgements

We thank the European Union's Horizon 2020 research and innovation programme under the Marie Sklodowska-Curie grant agreement N° 675417 (PET3D project) for financial support of the project and the studentship of I.P. We also thank the British Heart Foundation for the project grant PG/16/90/32518

Keywords: Fenretinide • Drug discovery • Radiopharmaceuticals • Cancer • Metabolic Syndrome.

[1] N. Mody, G.D. Mcilroy, *Biochemical Pharmacology* **2014**, *91* (3), 277–286.
[2] M.C. Chen, S.L. Hsu, H. Lin, T.Y. Yang, *BioMed* **2014**, 4 (4), 22.
[3] M.B. Sporn, N.M. Dunlop, D.L. Newton, W.R. Henderson, *Nature* **1976**, *263* (5573), 110–113.
[4] D. Delia, A. Aiello, L. Lombardi, P.G. Pelicci, F. Grignani, F. Formelli, S. Menard, A. Costa, U. Veronesi, *Cancer Res.* **1993**, *53* (24), 6036–6041.
[5] F. Preitner, N. Mody, T.E. Graham, O.D. Peroni, B.B. Kahn, *AJP: Endocrinology and Metabolism* **2009**, *297* (6), E1420–E1429.
[6] G.D. Mcilroy, M. Delibegovic, M.; C. Owen, P.N. Stoney, K.D. Shearer, P.J. McCaffery, N. Mody, *Diabetes* **2013**, *62* (3), 825–836.
[7] G.D. Mcilroy, S.R. Tammireddy, B.H. Maskrey, L. Grant, M.K. Doherty, D.G. Watson, M. Delibegović, P.D. Whitfield, N. Mody, *Biochemical Pharmacology* **2016**, *100*, 86–97.
[8] Y.H. Zeidan, Y.A. Hannun, *Trends in Molecular Medicine* **2007**, *13* (8), 327–336.
[9] C. Geng, H. Xu, Y. Zhang, X. Liu, F. Fang, Y. Chang *et al. Sci China Life Sci* **2017**, *60* (11), 1234-1241.
[10] M. Sato, A. Hiragun, H.Mitsui. *Res. Commun.* **1980**, *95* (4), 1839-1845
[11] S.-J. Um, Y.-J. Kwon, H.-S. Han, S.H. Park, M.-S. Park, Y.-S. Rho, H.-S. Sin, *Chemical and pharmaceutical bulletin* **2004**, *52* (5), 501–506.
[12] S.M. Mershon, A.L. Anding, J.S. Chapman, M. Clagett-Dame, L.A Stonerock, R.W. Curley, *Bioorganic & Medicinal Chemistry Letters* **2007**, *17* (3), 836–840.
[13] P. Tiberio, E. Cavadini, L. Cleris, S. Dallavalle, L. Musso, M.G. Daidone, V. Appierto. *Frontiers in Pharmacology* **2017**, *8* (226), 1-11.
[14] B.C. Das, M.E. Smith, G.V. Kalpana, Bioorganic *& Medicinal Chemistry Letters* **2008**, *18*, 3805-3808.
[15] A.L. Sabichi, H. Xu, S. Fischer, Z. Changchan, X. Yang, V.E. Steele, G.J. Kelloff, R. Lotan, J.L. Clifford, *Clinical Cancer Research* **2003**, *9*, 4606-4613.
[16] A.L. Anding, N.J. Nieves, V.V. Abzianidze, M.D. Collins, R.W. Curley, M. Clagett-Dame, *Chem. Res. Toxicol* **2011**, *24*, 1853-1861.
[17] M. Anzaldi, M. Viale, C. Macciò, P. Castagnola, V. Olivieri, C. Rosano, A. Balbi, *Cancer Chemother Pharmacol* **2017**, *79*, 725-736.
[18] R. Alvarez, B. Vaz, H. Gronemeyer, A.R. de Lera, *Chem. Rev.* **2014**, *114*, 1-125.
[19] J.A. Campos-Sandoval, C. Redondo, G.K. Kinsella, A. Pal, G. Jones, C.S. Eyre, S.C. Hirst, J.B.C Findlay, *J. Med. Chem.* **2011**, *54*, 4378-4387.
[20] A. Mariotti, E. Marcora, G. Bunone, A. Costa, U. Veronesi, M.A. Pierotti, G.D. Valle, *N J Natl Cancer Inst* **1994**, *86* (16), 1245–1247.
[21] H.J. Kim, N. Chakravarti, N. Oridate, C. Choe, F.X. Claret, R. Lotan, *Oncogene* **2006**, *25* (19), 2785–2794.
[22] I. Orienti, V. Salvati, G. Sette, M. Zucchetti, L. Bongiorno-Borbone, A. Peschiaroli, L. Zolla, F. Francescangeli, M. Ferrari, C. Matteo, *et al*. *J Exp Clin Cancer Res* **2019**, *38* (1), 373.
[23] J.R. Dunetz, J. Magano, G.A. Weisenburger. *Organic Process Research & Development* **2016**, *20* (2), 140–177.
[24] A.B. Barua, H.C. Furr. *Humana Press: Totowa, NJ*, **1998**; 3–28.
[25] C.D. Hein, X.M Liu, D. Wang. *Pharm Res* **2008**, *25* (10), 2216–2230.
[26] E. Bonandi, M.S. Christodoulou, G. Fumagalli, D. Perdicchia, G. Rastelli, D. Passarella, *Drug Discovery Today* **2017**, *22* (10), 1572–1581.
[27] D.S. Hill, S. Martin, J.L. Armstrong, R. Flockhart, J.J. Tonison, D.G. Simpson, M.A. Birch-Machin, C.P.F. Redfern, P.E. Lovat, *Clin Cancer Res* **2009,** *15* (4), 1192–1198.
[28] N. Hail, H.J. Kim, R. Lotan, Apoptosis **2006**, *11* (10), 1677–1694.
[29] C.M. Oslowski, F. Urano, *Meth. Enzymol.* **2011**, *490*, 71–92.
[30] J.M. Kraveka, L. Li, Z.M. Szulc, J. Bielawski, B. Ogretmen, Y.A. Hannun, L.M. Obeid, A. Bielawska, *J Biol Chem.* **2007**, *282* (23): 16718–16728.
[31] M. Rahmaniyan, R.W. Curley, L.M. Obeid, Y.A. Hannun, J.M. Kraveka, *Journal of Biological Chemistry* **2011**, *286* (28), 24754–24764.
[32] B.W. Parks, E. Nam, E. Org, E. Kostem, F. Norheim, S.T. Hui, C. Pan, M. Civelek, C.D. Rau, B.J. Bennett, *et al. Cell Metab* **2013**, *17* (1), 141–152.
[33] L. Aurelio, C.V. Scullino, M.R. Pitman, A. Sexton, V. Oliver, L. Davies, R.J. Rebello, L. Furic, D.J Creek, S.M. Pitson, *et al. J. Med. Chem.* **2016**, *59* (3), 965–984.
[34] F. Cingolani, M. Casasampere, P. Sanllehí, J. Casas, J. Bujons, G. Fabrias, *J Lipid Res* **2014**, *55* (8), 1711–1720.
[35] D. Van der Born, A. Pees, A.J. Poot, R.V.A. Orru, A.D. Windhorst, D.J. Vugts, *Chem. Soc. Rev.* **2017**, *46* (15), 4709–4773.
[36] P.J.H. Scott, B.G. Hockley, H.F. Kung, R. Manchanda, W. Zhang, M.R. Kilbourn, *Applied Radiation and Isotopes* **2009,** *67* (1), 88–94.
[37] K. Suzuki, O. Inoue, K. Tamate, F. Mikado, *Applied Radiation and Isotopes* **1990**, *41*, 593–599.
[38] R.M. Badwin, R.B. Innis, *et al.* M. *Nuclear Medicine and Biology* **1995**, *22*, 659–665.
[39] A. Bogni, E. Bombardieri, R. Iwata, L. Cadini, C. Pascali, *Journal of Radioanalytical and Nuclear Chemistry* **2003**, *256* (2), 199–203.
[40] T. Fukumura, R. Nakao, M. Yamaguchi, K. Suzuki, *Applied Radiation and Isotopes* **2004**, *61* (6), 1279–1287.
[41] R.M. Fawdry, *Applied Radiation and Isotopes* **2007**, 65 (11), 1193–1201.
[42] M. Woods, L. Leung, K. Frantzen, J.G. Garrick, Z. Zhang, C. Zhang, W. English, D. Wilson, F. Bénard, K.-S. Lin, *EJNMMI radiopharm. chem.* **2017**, *2* (1), 13.

[43] K. Nieto, P. Pei, D. Wang, S.R. Mallery, S.P. Schwendeman. *Int. J. Pharm.* **2018**, *538* (1-2), 48-56.

[44] A.D. Windhorst, T.T. Linden, A. de Nooij, J.F. Keus, F.L. Buijs, P.E. Schollema, L.F. van Rooij, J.D.M. Herscheid, *J Label Compd Radiopharm* **2001**, *44* (S1), S1052–S1054.

[45] H. Ganin, J. Rayo, N. Amara, N. Levy, P. Krief, M.M. Meijler, *Med. Chem. Commun.* **2012**, *4* (1), 175–179.

Table of Contents

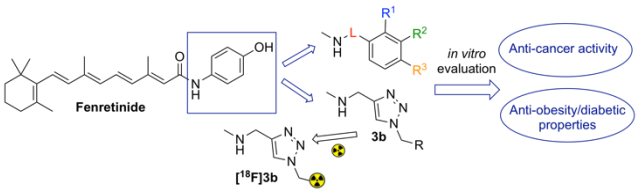

A library of fenretinide analogues has been designed and synthesised by using a single step amide coupling or a click-chemistry approach. The compounds synthesised were then evaluated *in vitro* to assess their anti-cancer activity and their anti-obesity/diabetic properties. Based on the positive *in vitro* results, the click-type analogue **3b** was then selected as potential PET imaging tracer and the radiosynthesis of [^{18}F]**3b** was performed. The tracer was insufficiently stable for *in vivo* imaging, owing to radiolytic decomposition.